

Computation of the Magnetic Field and Vorticity in Heavy-Ion Collisions

Wei-Tian Deng (邓维天)

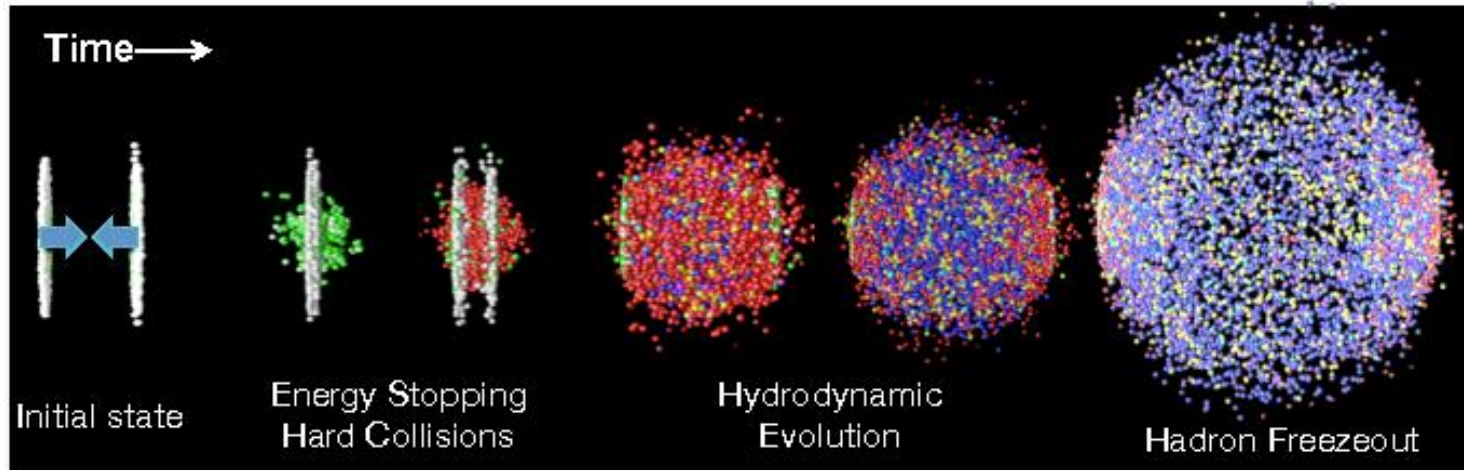
(Huazhong University of Science and Technology)

Outlook

- Electromagnetic (EM) fields in HIC
[Phys.Rev. C85 \(2012\) 044907 / WTD, X-G Huang](#)
- Background Vs. CME effect
[Phys.Lett. B742 \(2015\) 296-302 / WTD, X-G Huang](#)
[Phys.Rev. C94 \(2016\) 041901 / WTD, X-G Huang, G-L Ma, G Wang](#)
- Vorticity in HIC
[Phys.Rev. C93 \(2016\) no.6, 064907 / WTD, X-G Huang](#)

Electromagnetic (EM) fields in HIC

Motivation

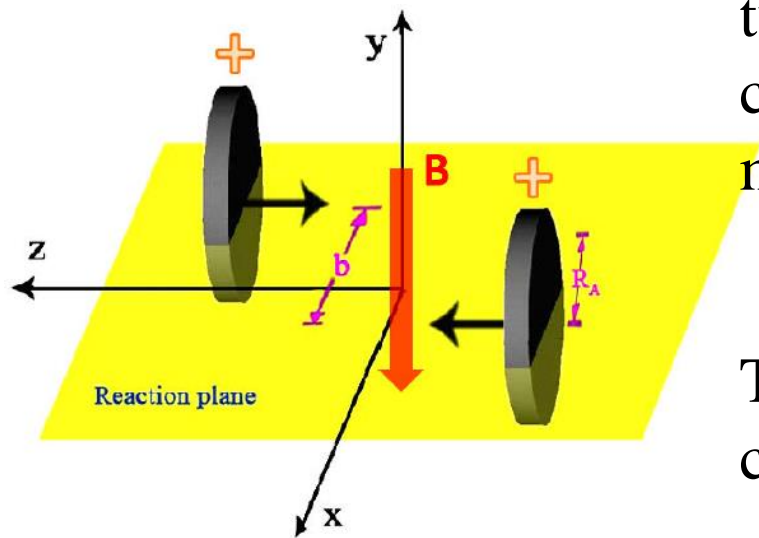


Due to fast, oppositely directed motion of two colliding ions, off-central heavy-ion collisions can create strong transient magnetic fields.

[J.Rafelski and B.Muller, Phys.Rev.Lett.36,517](#)

The magnetic fields generated in Au+Au collisions at RHIC can reach $\sim 10^{19}$ Gauss

[D.E.Kharzeev, L.D.McLerran, and H.J.Warringa, Nucl.Phys.A 803,227](#)



Such a strong B field may influence the dynamics of QGP

Chirality imbalance + magnetic field = chiral magnetic effect (CME)

Kharzeev 2004, Kharzeev, McLerran, Warringa, Fukushima 2007-2008

Chiral Magnetic Effect (CME) \Rightarrow Charge separation

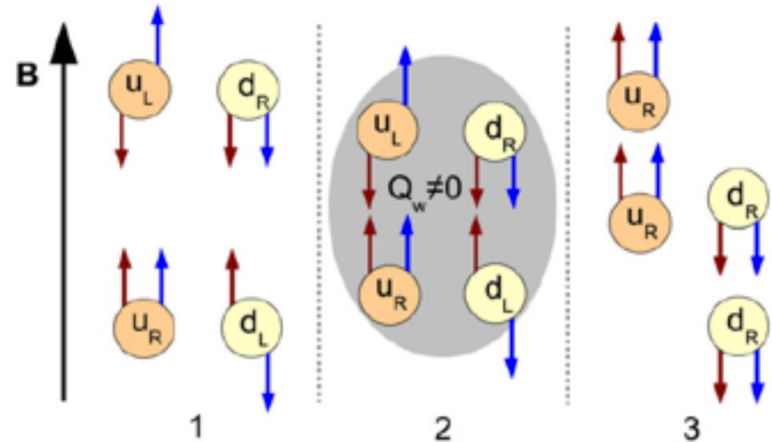
$$\vec{J} = \sigma_5 \vec{B}$$

chiral conductivity

$$\sigma_5 = N_c \sum_f \frac{q_f^2 \mu_5}{2\pi^2}$$

with axial or chiral chemical potential

$$\mu_5 = \frac{\mu_R - \mu_L}{2}$$

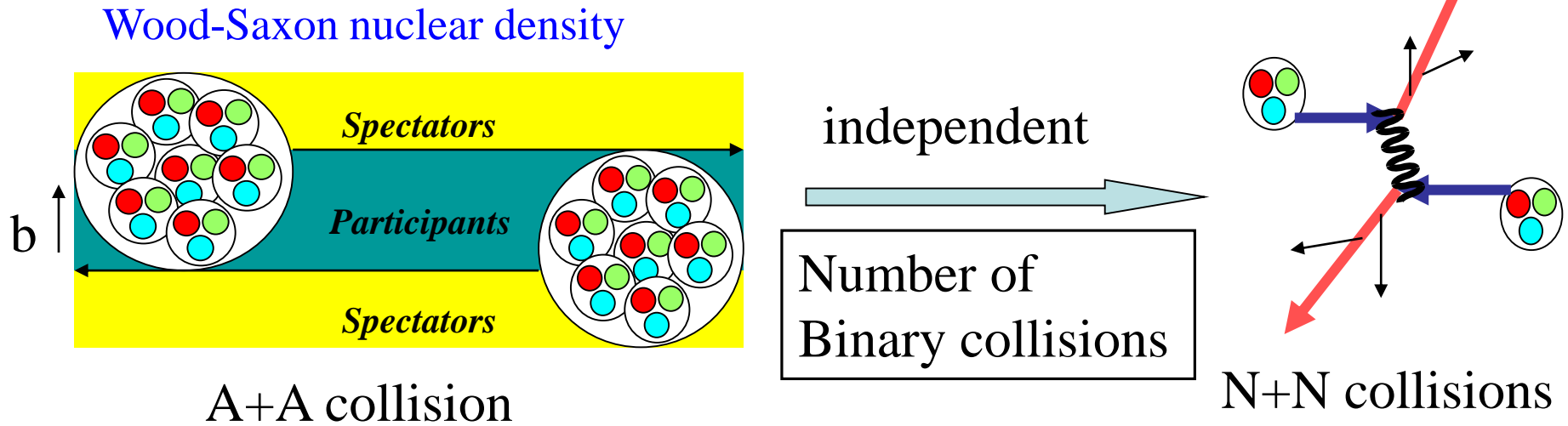


Motivation for EM in A+A

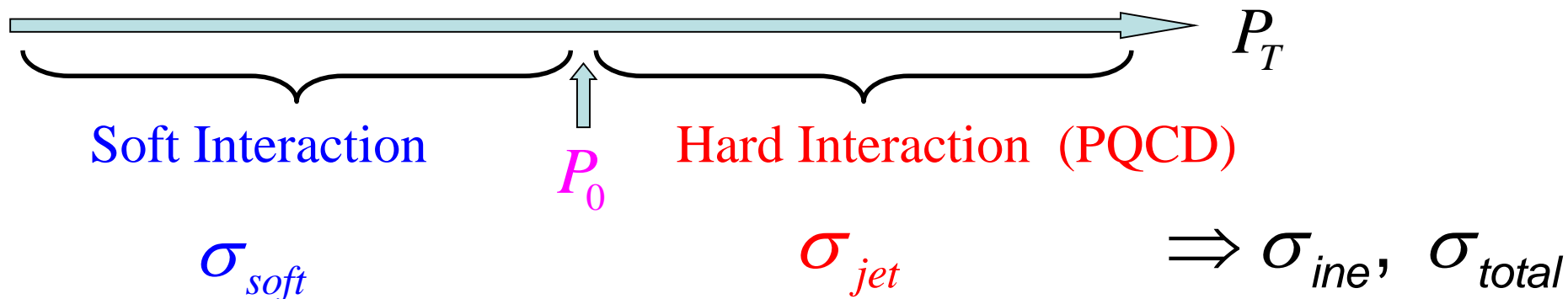
- Most study of the field strength so far are based on the averaging over events. Then only B_y remains sizable.
- However, many effects should be based on the event-by-event analysis, and depended on the space-time distribution of the field.
- So, in this work, we give a detailed study of EM field in heavy-ion collisions on the e-b-e bases using HIJING model.

HIJING Model

Binary Collision Approximation




Two-Component Model in N-N Collisions



Initial Kinematics of Nucleon

In the rest frame of Nucleus:

Spherical Woods-Saxon nuclear distribution $\rho(r) = \frac{\rho_0}{1 + \exp[(r - R_A)/a]}$

 (x_N, y_N, z_N) of each nucleon (proton)

In the center-of-mass frame:

$$E = \sqrt{s} / 2$$

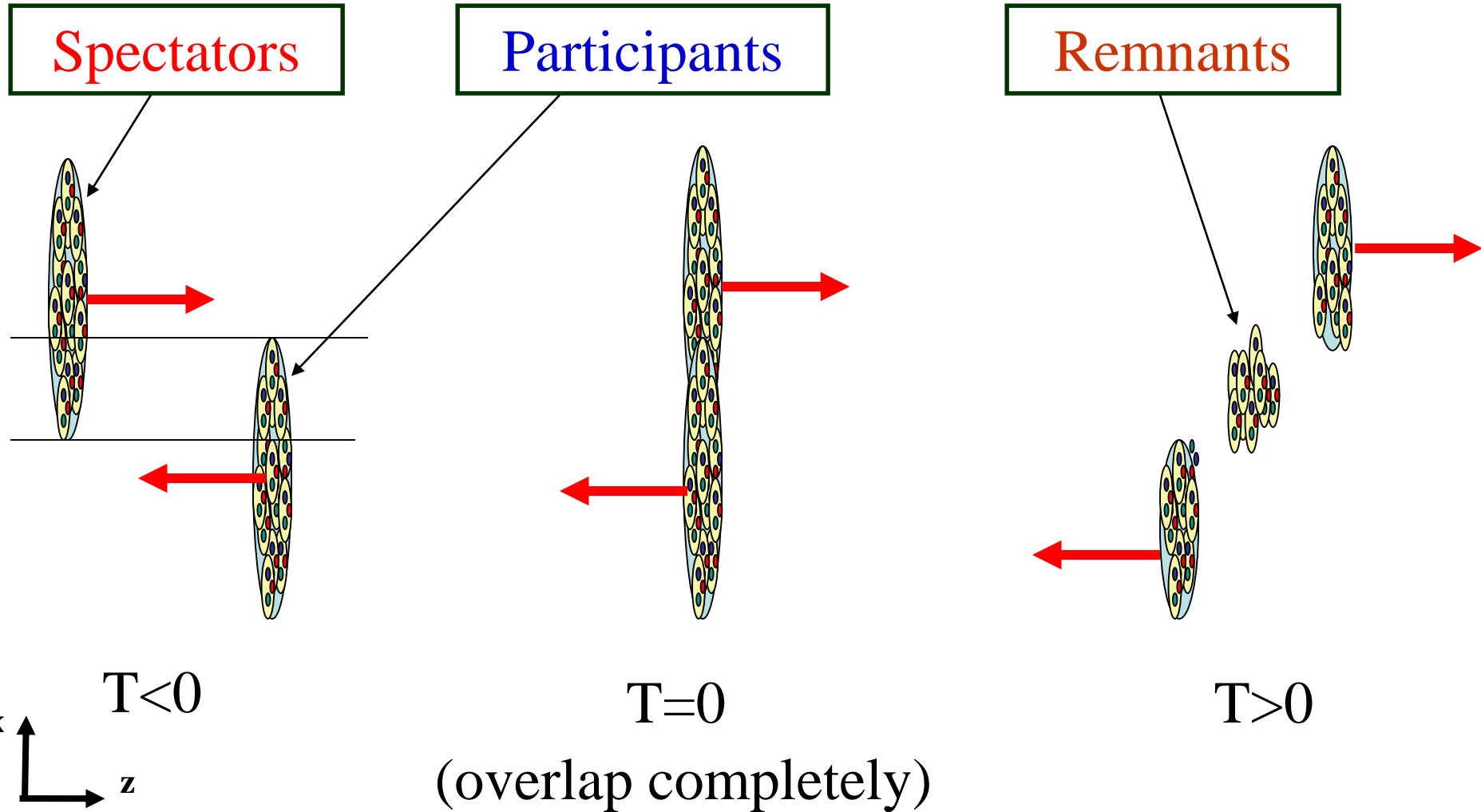
$$v_z^2 = 1 - (2m_N / \sqrt{s})^2, \quad v_x = v_y = 0$$

m_N is the rest mass of nucleon

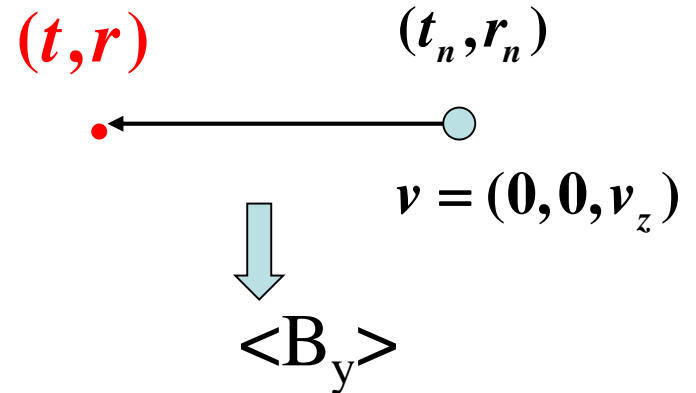
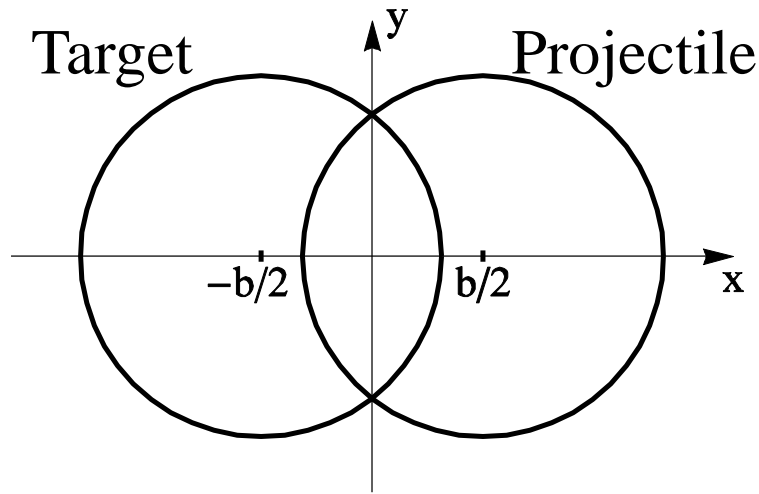
$$\Rightarrow z_N^{\text{Lorentz}} = z_N \frac{2m_N}{\sqrt{s}}$$

Lorentz Contraction

Time definition in HIC



Lienard-Wiechert potential



$$e\mathbf{E}(t, \mathbf{r}) = \frac{e^2}{4\pi} \sum_n Z_n \frac{\mathbf{R}_n - R_n \mathbf{v}_n}{(R_n - \mathbf{R}_n \cdot \mathbf{v}_n)^3} (1 - v_n^2)$$

$$e\mathbf{B}(t, \mathbf{r}) = \frac{e^2}{4\pi} \sum_n Z_n \frac{\mathbf{v}_n \times \mathbf{R}_n}{(R_n - \mathbf{R}_n \cdot \mathbf{v}_n)^3} (1 - v_n^2)$$

Relative position $\mathbf{R}_n = \mathbf{r} - \mathbf{r}_n$

with retarded condition $t_n = t - |\mathbf{r} - \mathbf{r}_n|$

Event-by-Event Analysis

On event-averaged basis:

Because of the symmetry,
only B_y is non-zero.

$$\langle B_x \rangle, \langle B_y \rangle, \langle E_x \rangle, \langle E_y \rangle$$

$$\langle B_x \rangle \approx 0, \langle B_z \rangle = 0$$

$$\langle E_x \rangle \approx \langle E_y \rangle \approx \langle E_z \rangle \approx 0$$

On event-by-event basis:

because of the fluctuation of proton's position,
 E_x , E_y and B_x may be non-vanished.

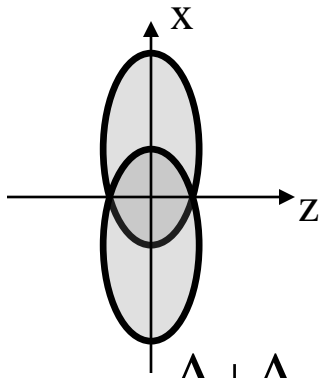
$$\langle |B_x| \rangle, \langle |B_y| \rangle, \langle |E_x| \rangle, \langle |E_y| \rangle$$

$$\langle |E_y| \rangle \approx \langle |B_x| \rangle$$

$$\langle |B_y| \rangle \geq \langle |E_x| \rangle$$

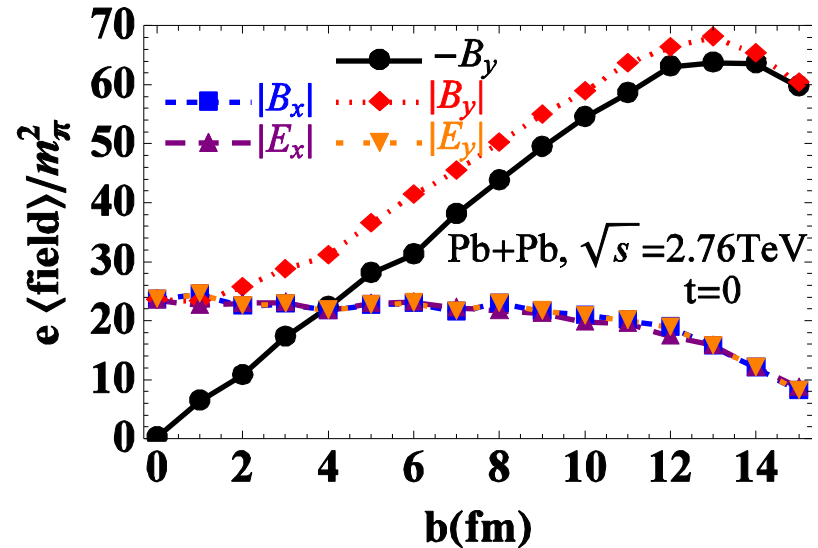
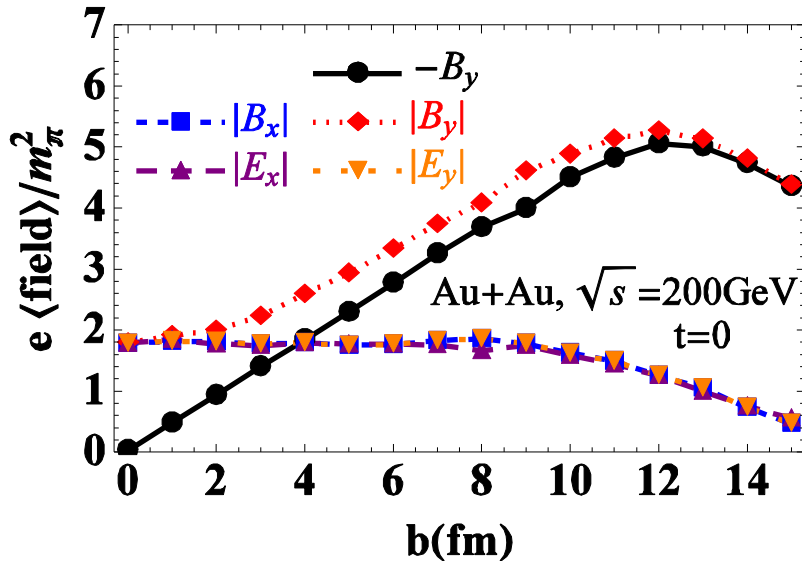
Numerical Results of EM Field

- For $t=0$, only **Spectators** and **Participants** contribute to the EM field.
 - b dependence
 - Energy dependence
 - Spatial distribution
- Time evolution of EM field at early stage

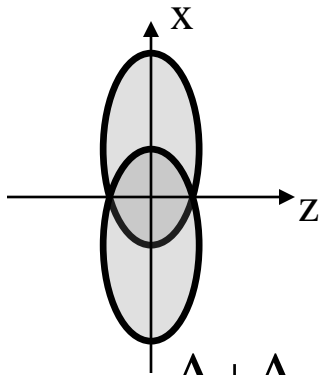


A+A, $t=0$, $\mathbf{r}=0$

b Dependence

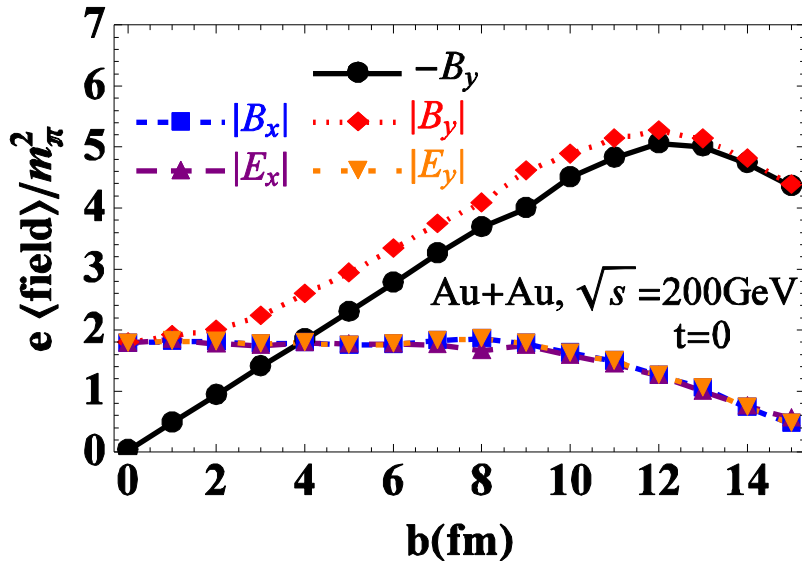


- On events-averaged basis, only B_y remains indeed
- On e-b-e basis, the B_x , E_x and E_y are approximately equivalent. And they are almost independent on the b .
- Higher energy \longrightarrow higher strength of field

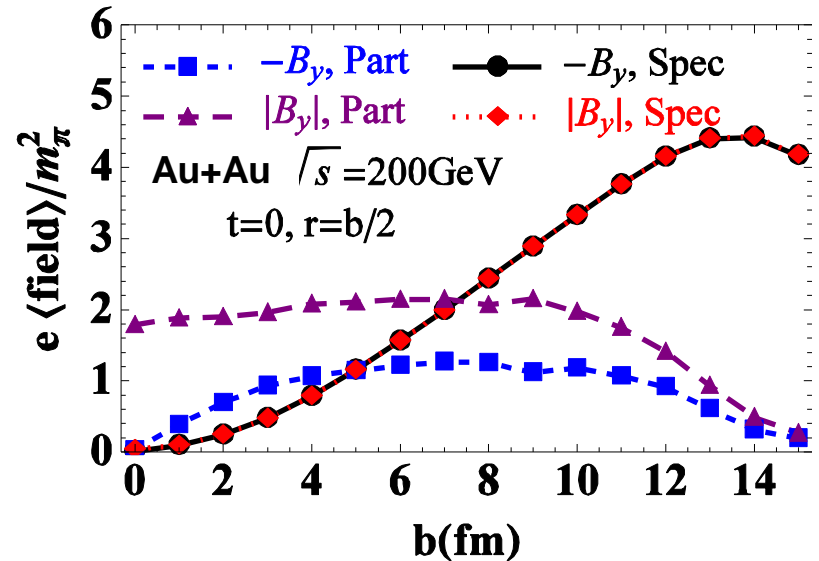


b Dependence

A+A, $t=0$, $\mathbf{r}=0$



Spectator Vs. Participant



- The difference of B_y and $|B_y|$ come from Participants.
- The B_y produced by Spectators in each event is with the same sign, that's why $B_y=|B_y|$ for Spectators
- The net B_y produced by Participants may be with different sign, so $B_y \leq |B_y|$ for Participants

Energy Dependence

$$e\mathbf{E}(t, \mathbf{r}) = \frac{e^2}{4\pi} \sum_n Z_n \frac{\mathbf{R}_n - R_n \mathbf{v}_n}{(R_n - \mathbf{R}_n \cdot \mathbf{v}_n)^3} (1 - v_n^2)$$

$$e\mathbf{B}(t, \mathbf{r}) = \frac{e^2}{4\pi} \sum_n Z_n \frac{\mathbf{v}_n \times \mathbf{R}_n}{(R_n - \mathbf{R}_n \cdot \mathbf{v}_n)^3} (1 - v_n^2)$$

As the field at $t=0$ are mainly caused by spectators and participants: $\mathbf{v}_z \rightarrow \mathbf{1}$

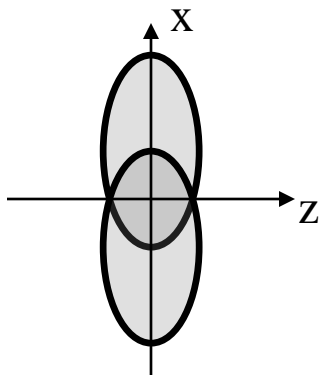
On the transverse plane:

$$e\mathbf{E}_\perp(0, \mathbf{r}) \approx \frac{e^2}{4\pi} \frac{\sqrt{s}}{2m_N} \sum_n \frac{\mathbf{R}_{n\perp}}{R_{n\perp}^3},$$

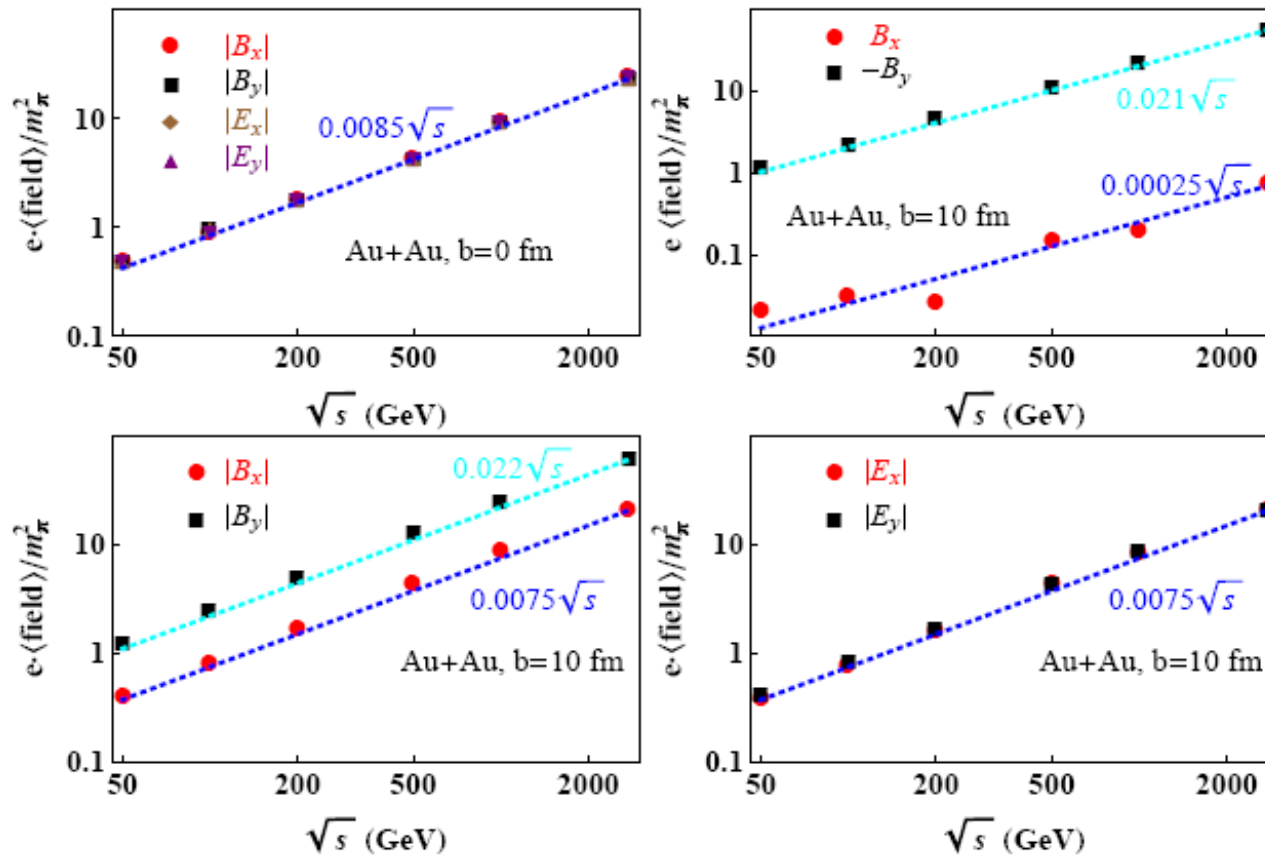
$$e\mathbf{B}_\perp(0, \mathbf{r}) \approx \frac{e^2}{4\pi} \frac{\sqrt{s}}{2m_N} \sum_n \frac{\mathbf{e}_{nz} \times \mathbf{R}_{n\perp}}{R_{n\perp}^3},$$

Linear dependence
on colliding energy



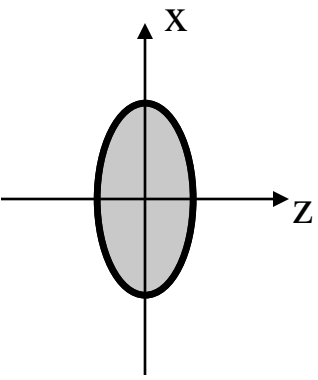


Energy Dependence



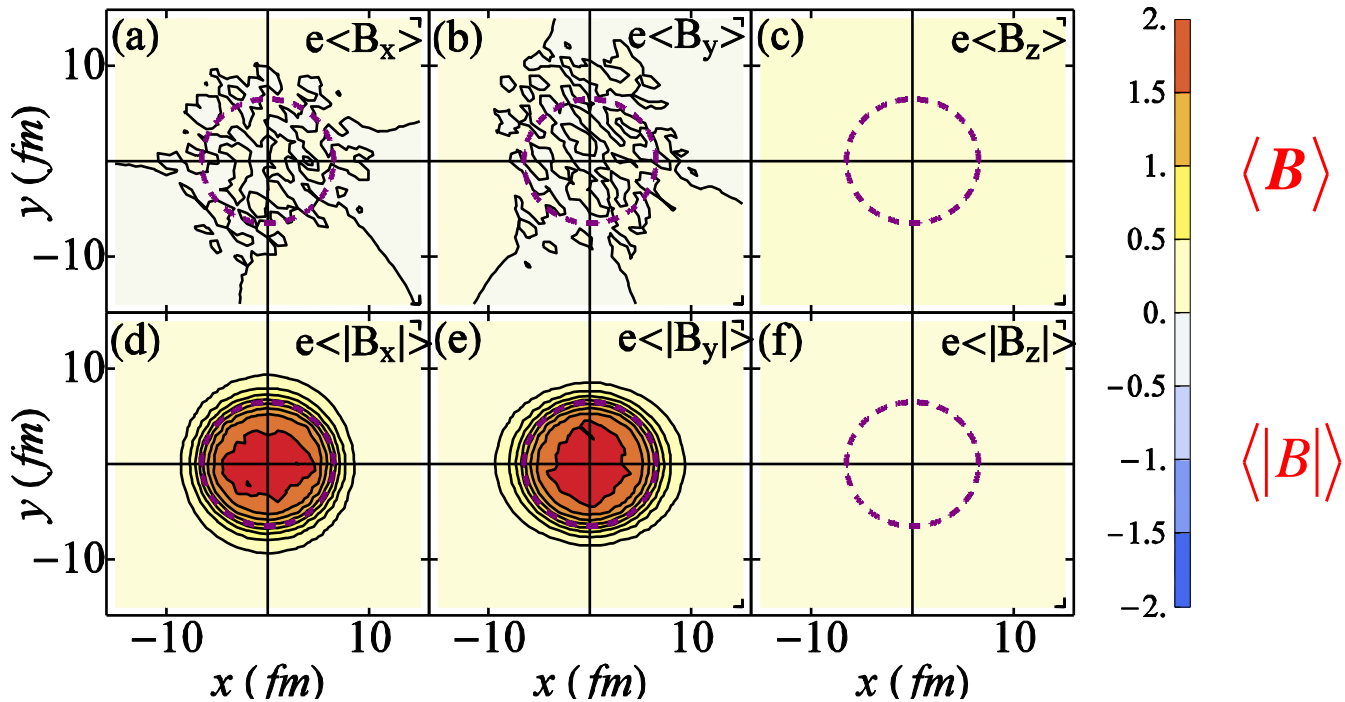
$t=0, \mathbf{r}=0$

$$e \cdot \text{Field} \propto \sqrt{s} \cdot f(b / R_A)$$

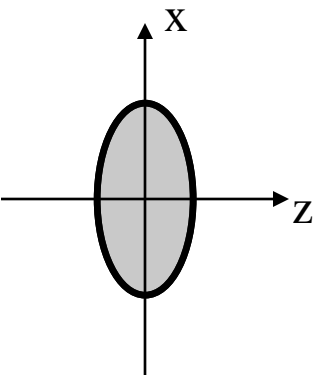


Spatial Distribution

$\sqrt{s}=200\text{GeV}$, $t=0$, $b=0$

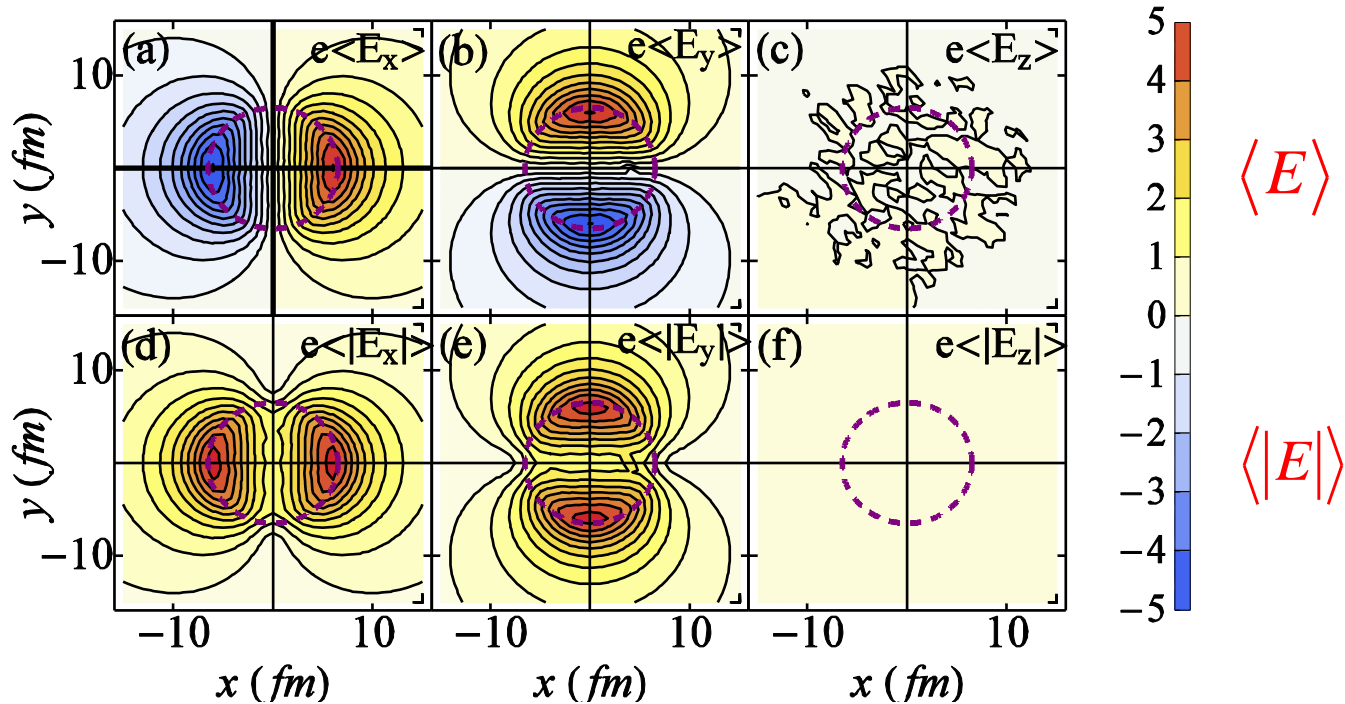


- B_x and B_y are approximately vanished at $b=0$ due to geometry symmetry.
- $|B_x|$ and $|B_y|$ are sizable and symmetry as a circle, and peak at $r=0$.

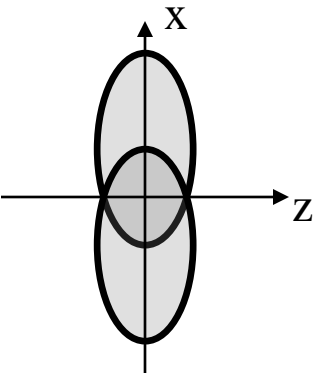


Spatial Distribution

$\sqrt{s}=200\text{GeV}$, $t=0$, $b=0$

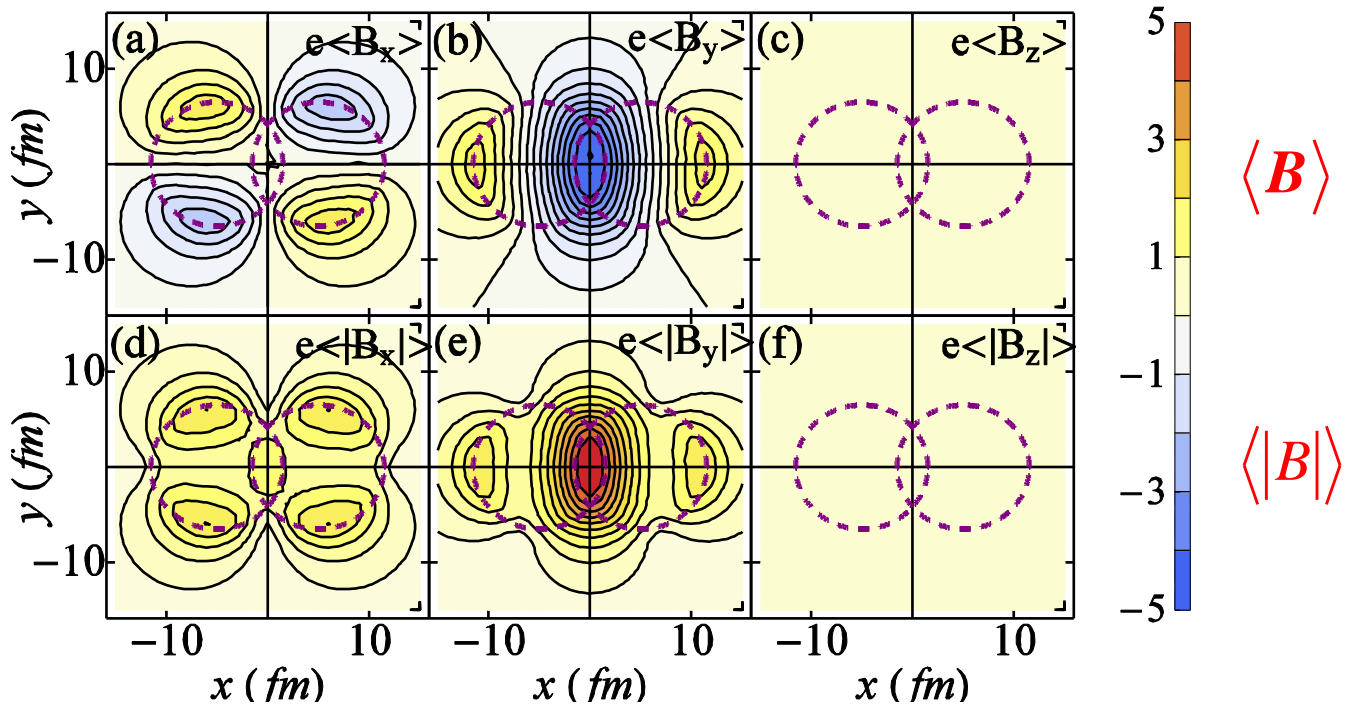


- The spatial distribution of E is quite different with B .
- For E_x and E_y , although they are vanished at center, but still sizable at other observation points, peak at circumference

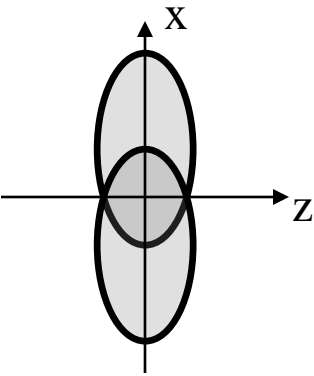


Spatial Distribution

$\sqrt{s}=200\text{GeV}$, $t=0$, $b=10\text{ fm}$

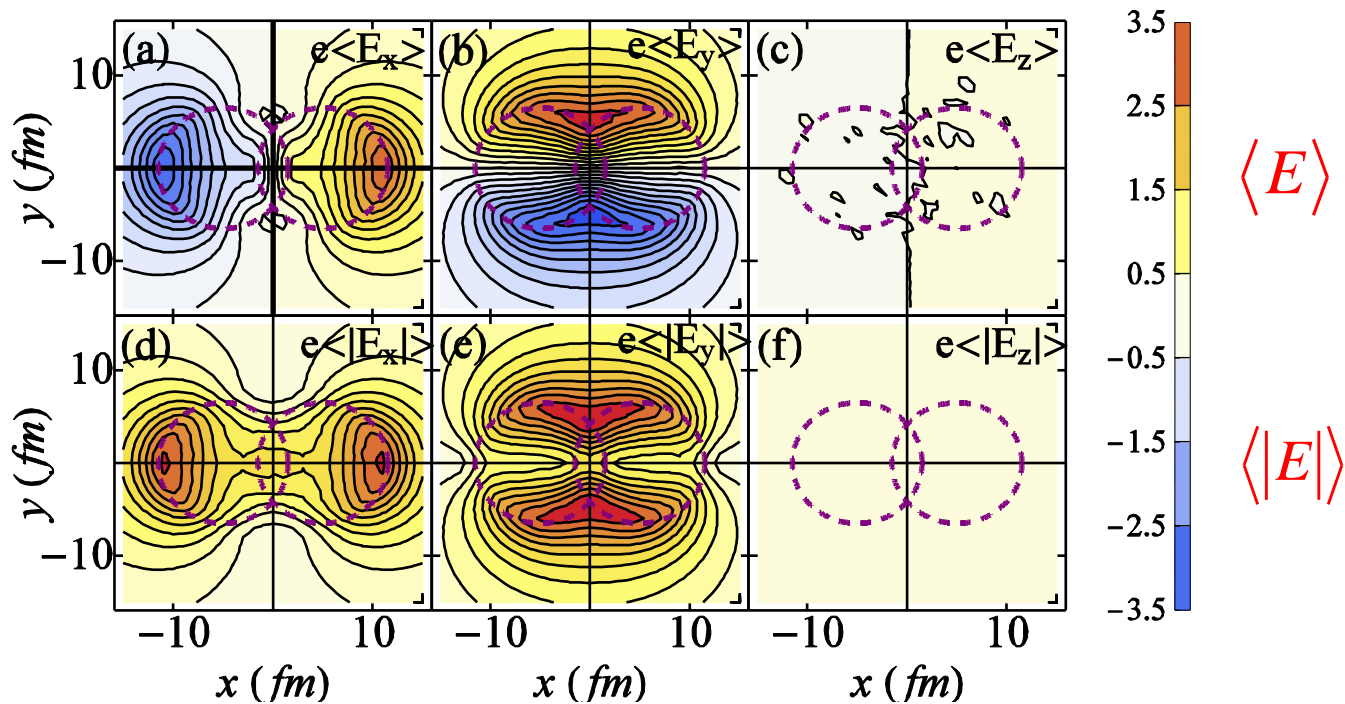


- For off-central A+A collisions, although $B_x=0$ at center, the spatial distribution has also structure.
- The distribution of fields distribute similarly like the fields come from two uniformly charged oppositely moving discs.



Spatial Distribution

$\sqrt{s}=200\text{GeV}$, $t=0$, $b=10\text{ fm}$



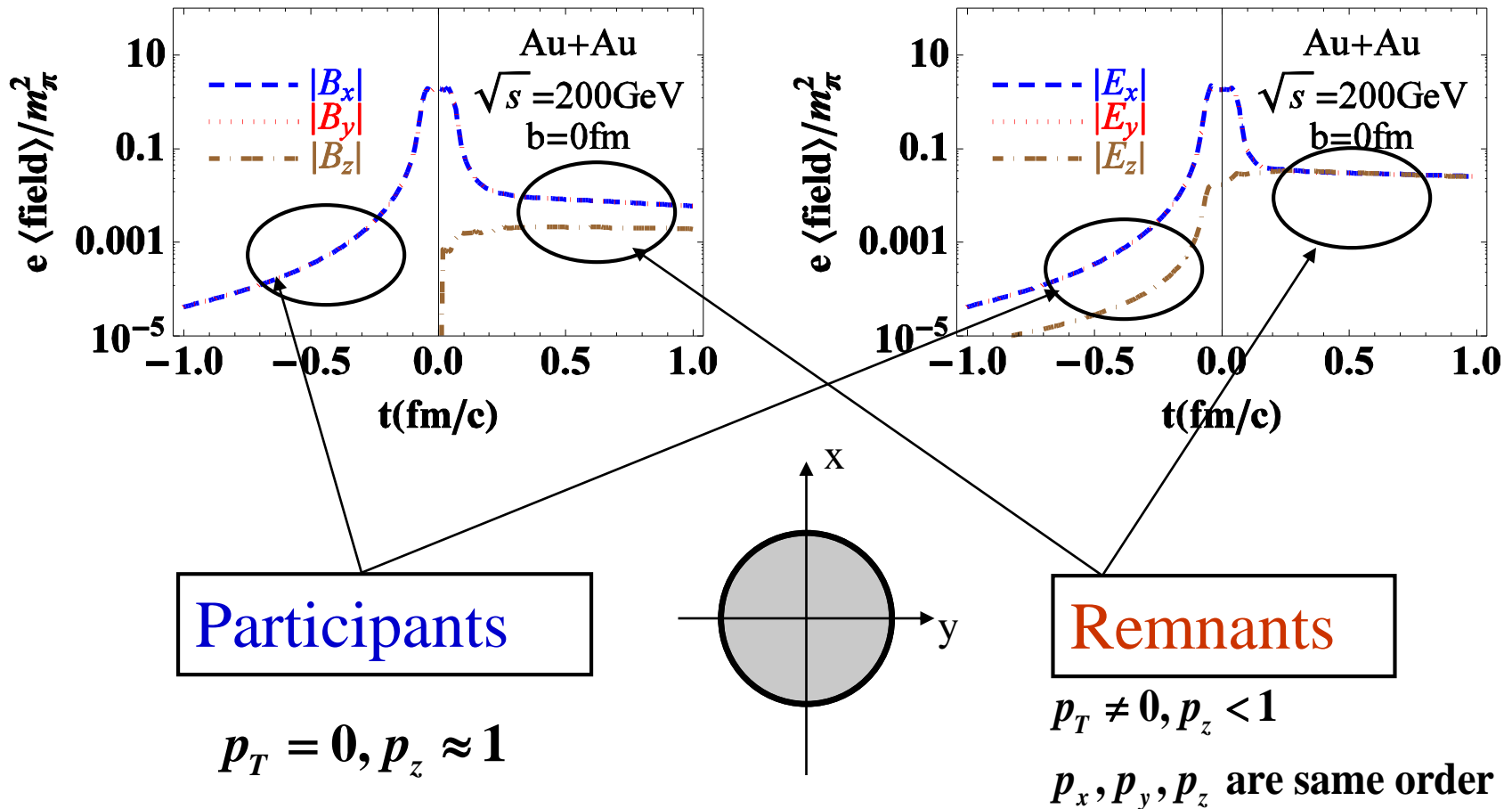
- For the events-averaged E_x and E_y , there is a large gradient in the overlap area. This maybe cause some observations, like the separation of charge parton in QGP.

Early-Stage time evolution of EM

- In our calculation, we neglect the contribution from produced partons (QGP)
 - The QGP are assumed as insulating medium
- We neglect the back response of field on the motion of nucleon.
 - So we only give the time evolution in early-stage i.e. before the formation of QGP.

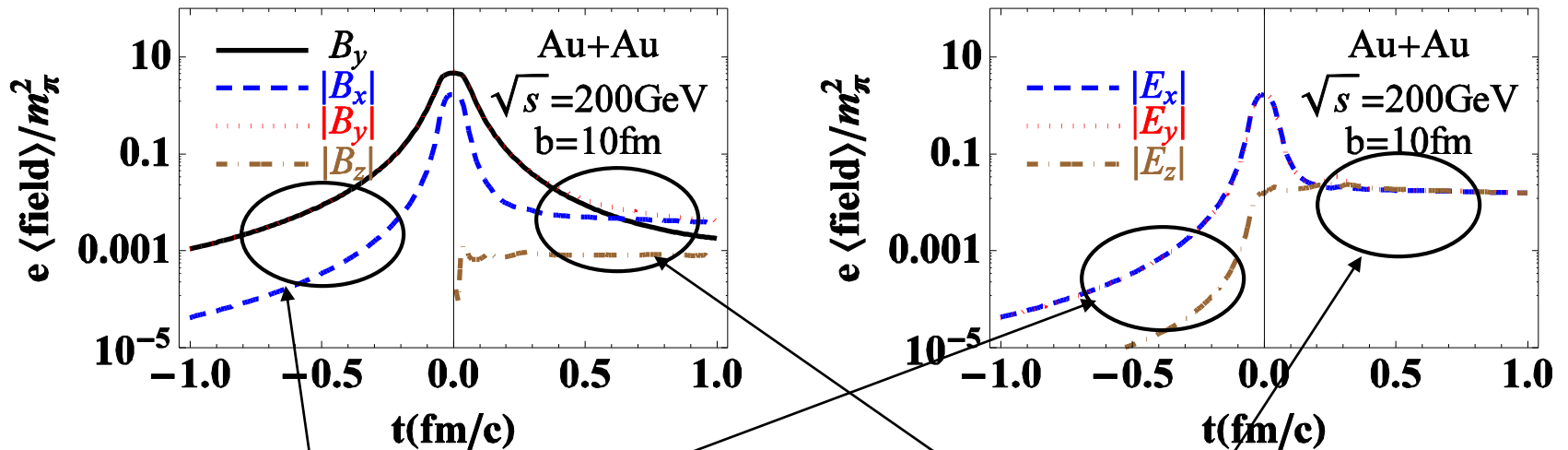
Early-Stage time evolution of EM

Au+Au, 200GeV, $r=0$, $b=0$



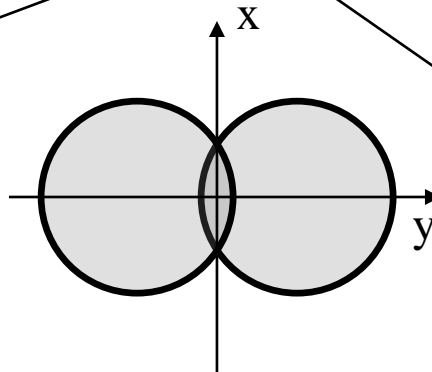
Early-Stage time evolution of EM

Au+Au, 200GeV, $r=0$, $b=10$ fm



Spectators

$$p_T = 0, p_z \approx 1$$



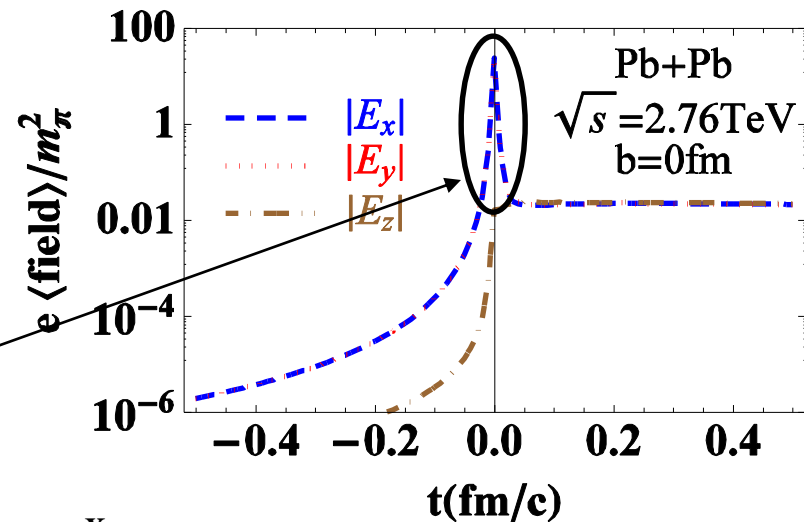
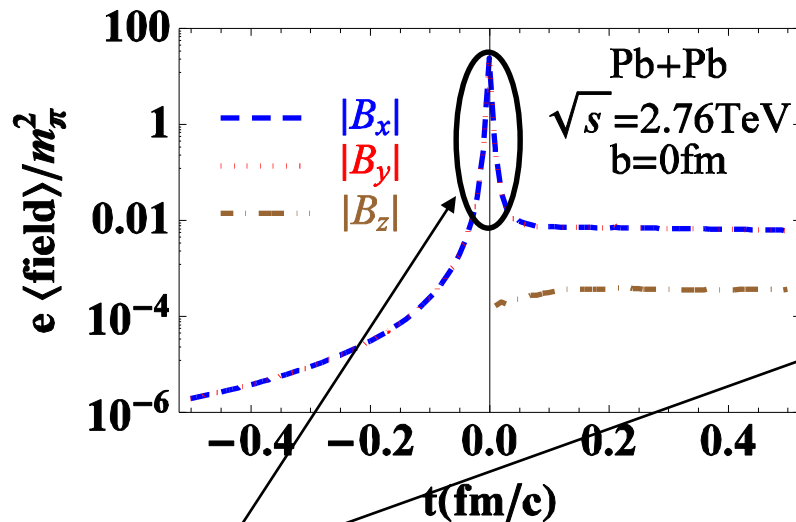
Remnants

$$p_T \neq 0, p_z < 1$$

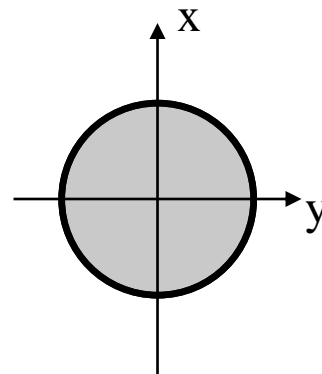
p_x, p_y, p_z are same order

Early-Stage time evolution of EM

Pb+Pb, 2.76TeV, $r=0$, $b=0$

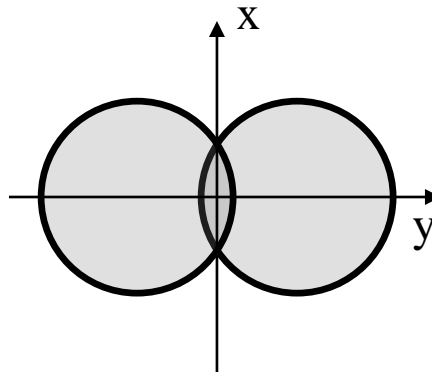
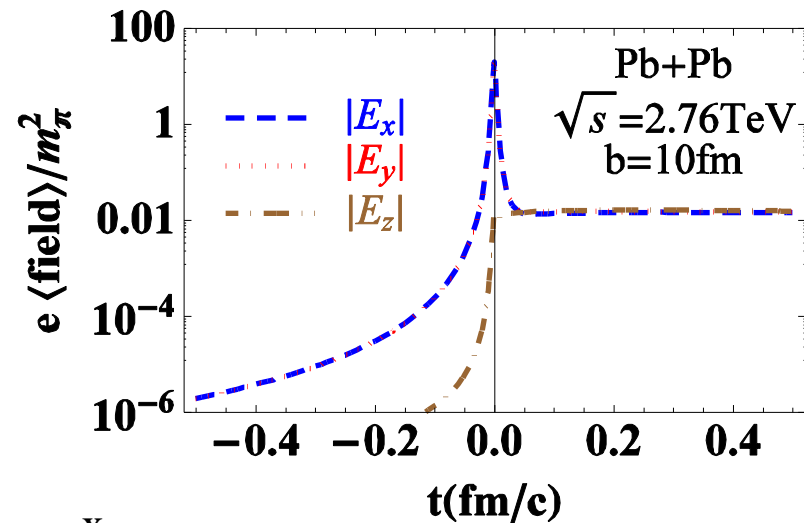
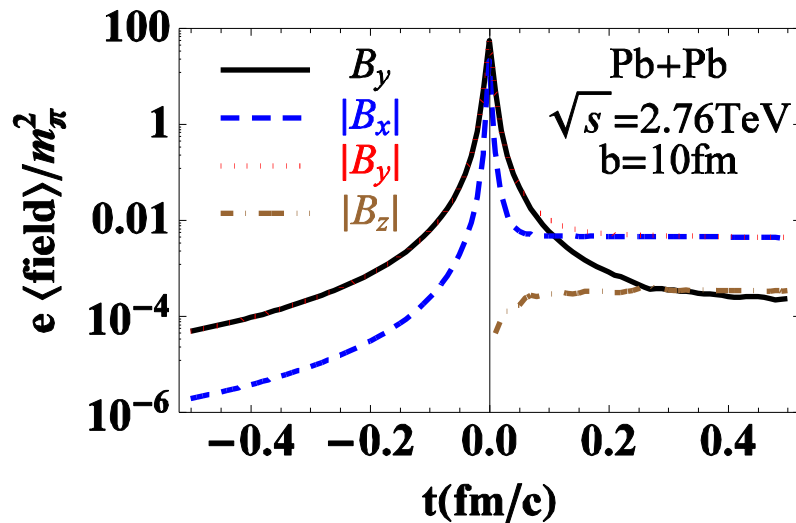


The sharp peaks are because of the larger v_z on higher energy. The nucleus approach and leave more quickly.



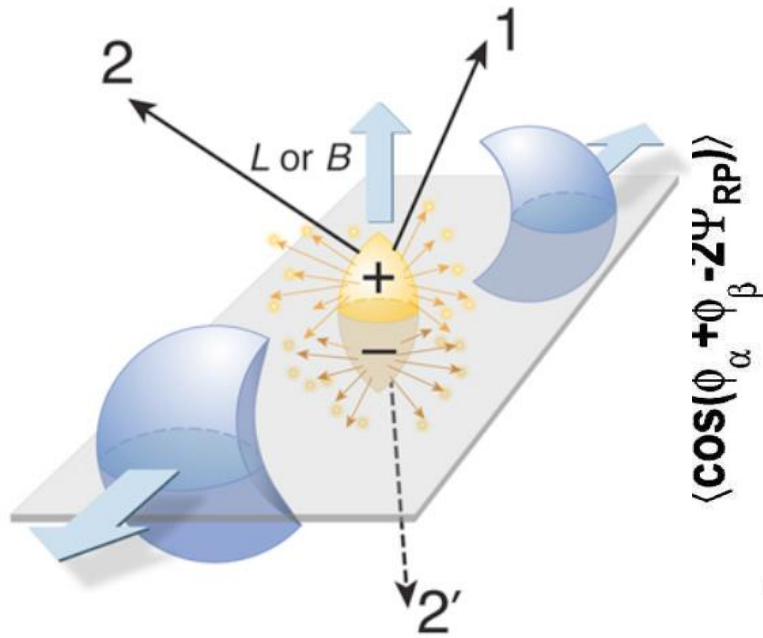
Early-Stage time evolution of EM

Pb+Pb, 2.76TeV, $r=0$, $b=10\text{fm}$

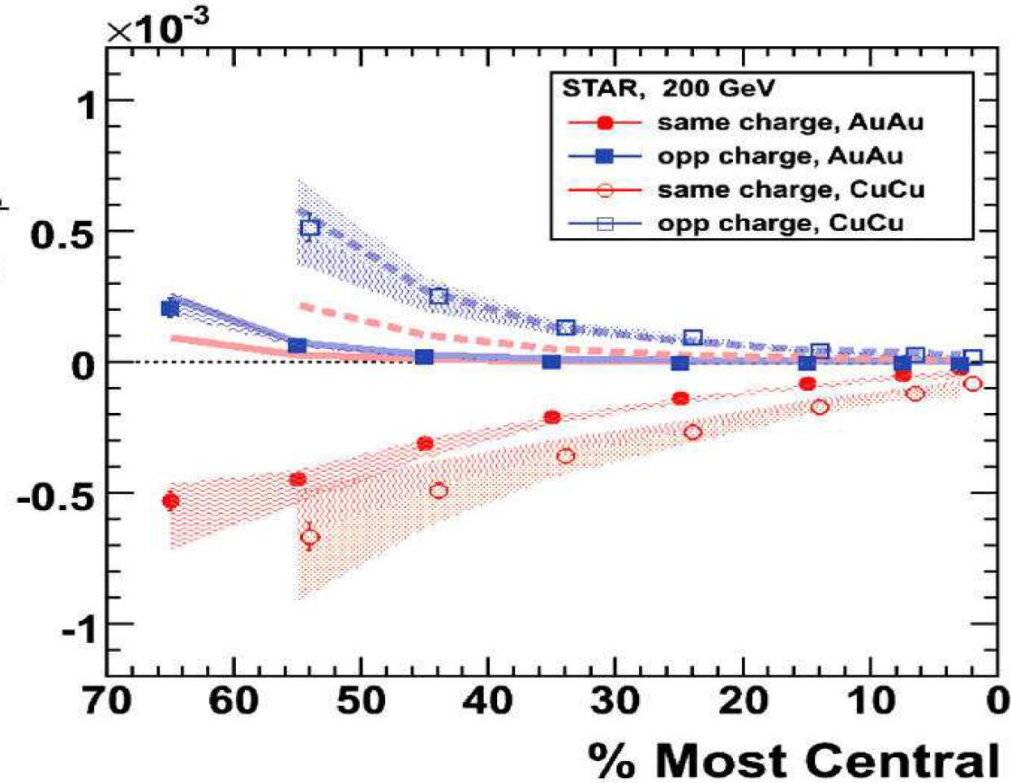


Background Vs. CME effect

Experiment searches of CME



charge correlation in Au+Au, Cu+Cu, and Pb+Pb are consistent with CME:



Two particle charge azimuthal correlation function:

$$\gamma_{q_1, q_2} = \langle \cos \phi_1 + \phi_2 - 2\psi_{RP} \rangle$$

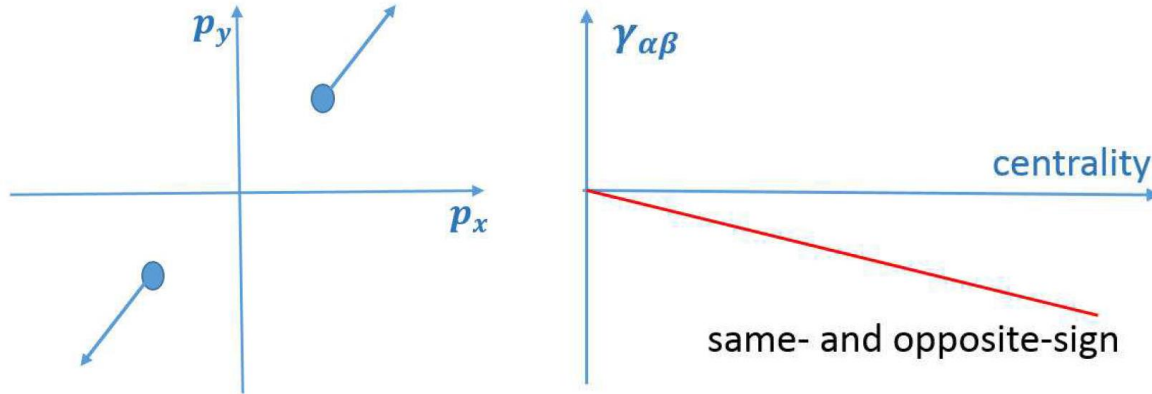
$$\gamma_{ss} = (\gamma_{++} + \gamma_{--}) / 2$$

$$\gamma_{os} = \gamma_{+-}$$

Possible background of $\langle \cos \phi_1 + \phi_2 - 2\psi_{RP} \rangle$

- Transverse momentum conservation (TMC) (Pratt, Schlichting, and Gavin, 2010; Liao, Bzdak, and Koch 2010)

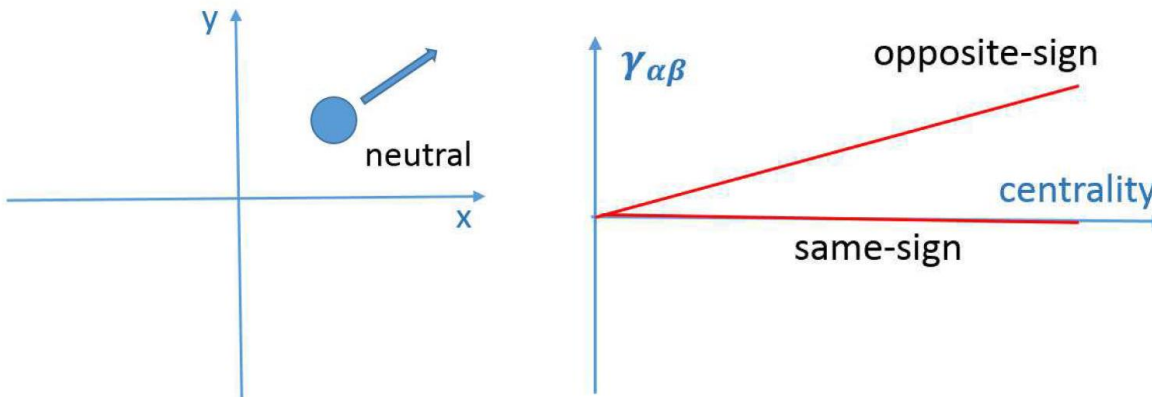
$$\sim -\frac{v_2}{N}$$



$$\Delta\gamma = \gamma_{os} - \gamma_{ss}$$

- Local charge conservation (Pratt and Schlichting, 2011)

$$\sim \frac{v_2}{N}$$



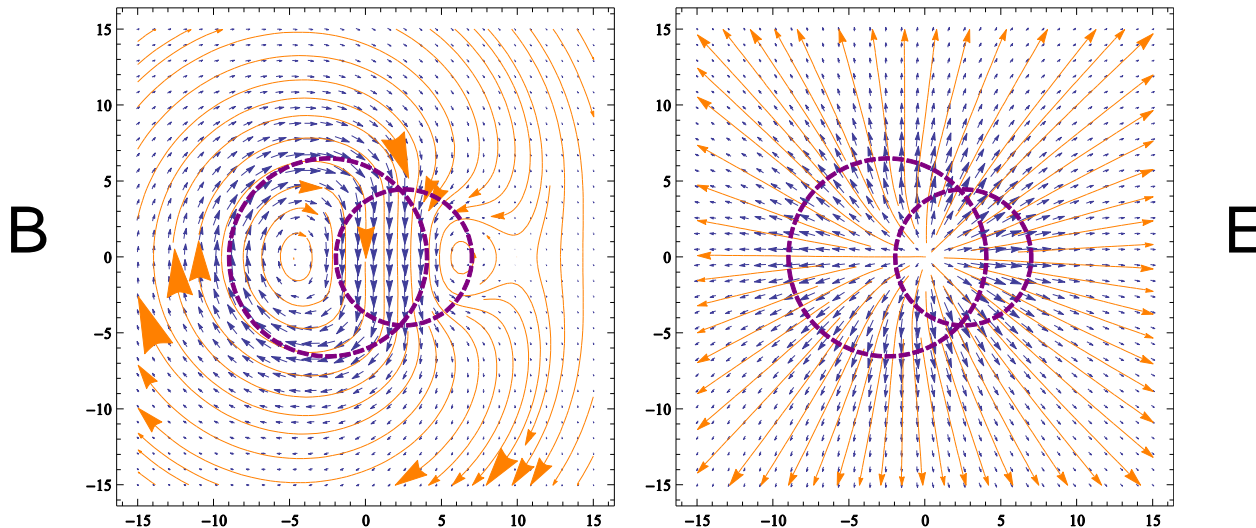
How to determine the CME-induced signals?

1, different **Size** collision: **Cu+Au**

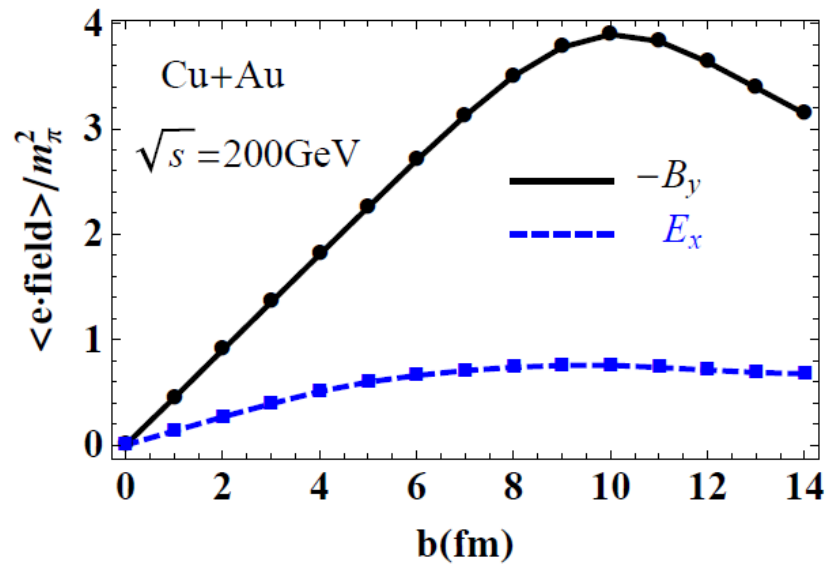
If **v2-driven** is dominant, the charge correlation



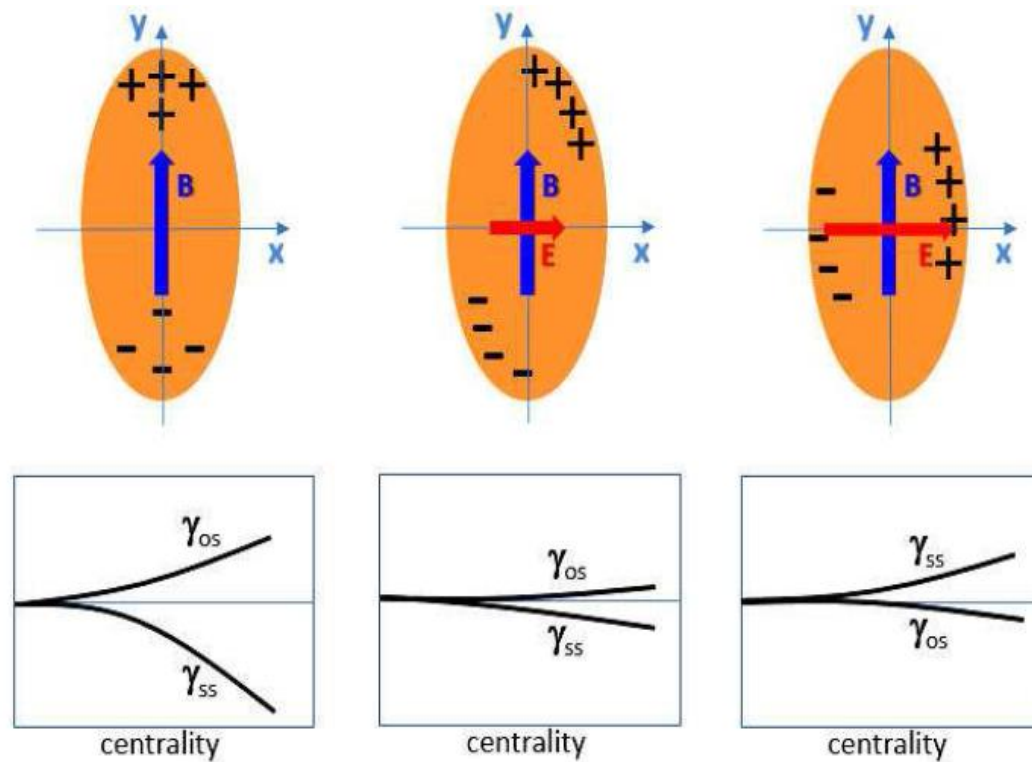
If **CME** is dominant, the charge correlation



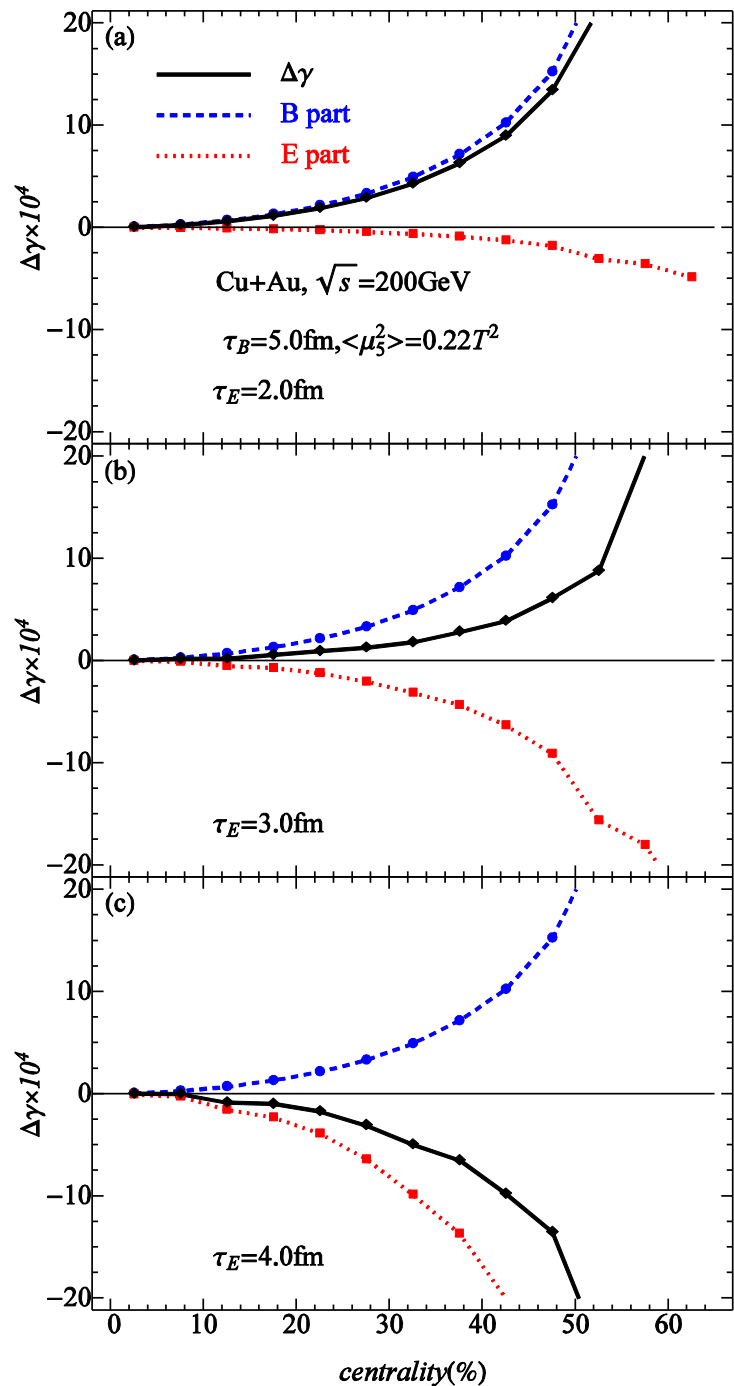
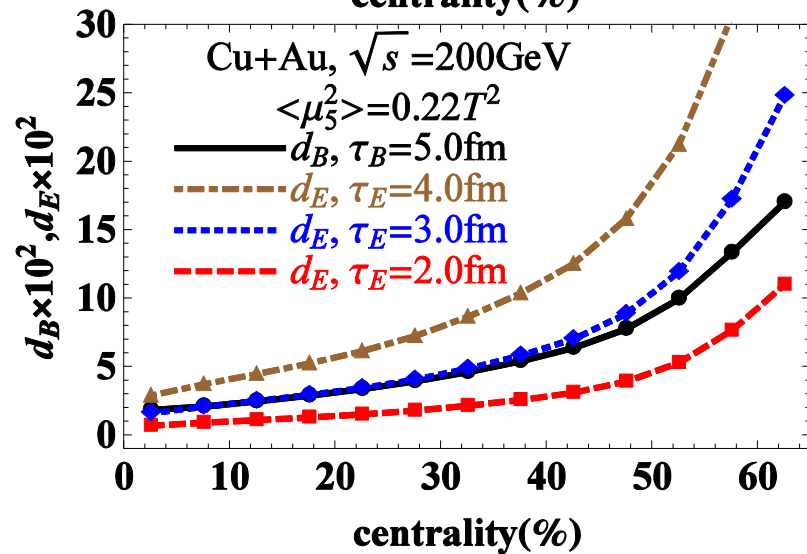
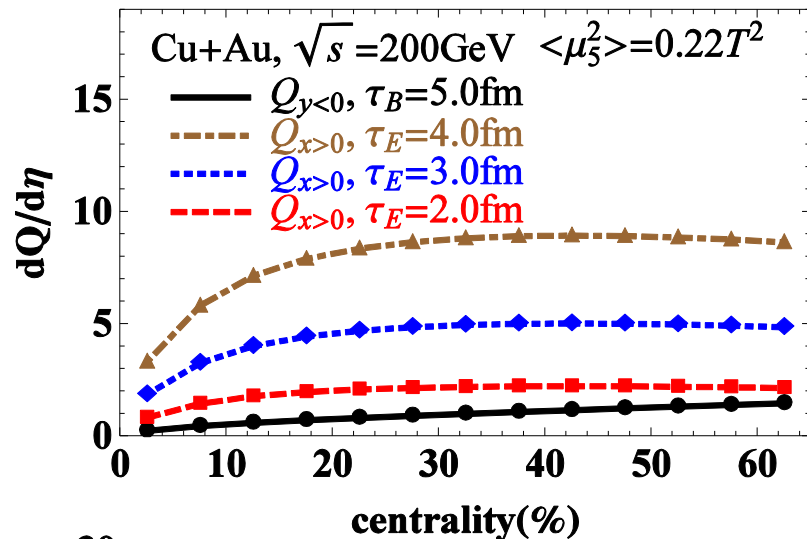
In transverse plane



If E field is strong enough,
 or its lifetime is long enough,



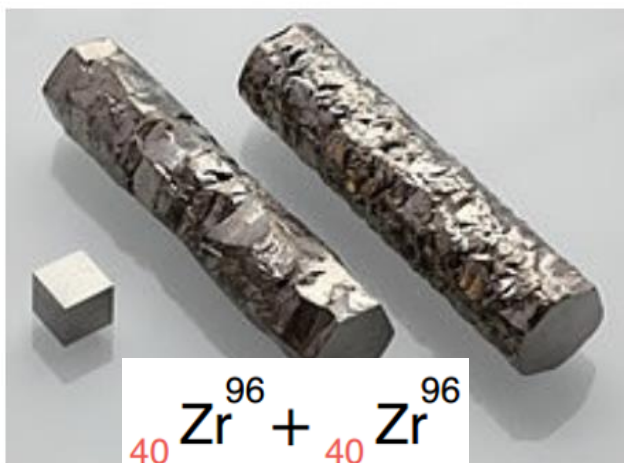
in general, the life time of E is shorter than B



2, Isobaric collision:

— $^{96}_{40}\text{Zirconium}$ vs $^{96}_{44}\text{Ruthenium}$

锆



钌



Same $A=96$ \longrightarrow Same elliptic flow
(via ϵ_2)

\longrightarrow v_2 -driven
background fixed

Different Z \longrightarrow different B field

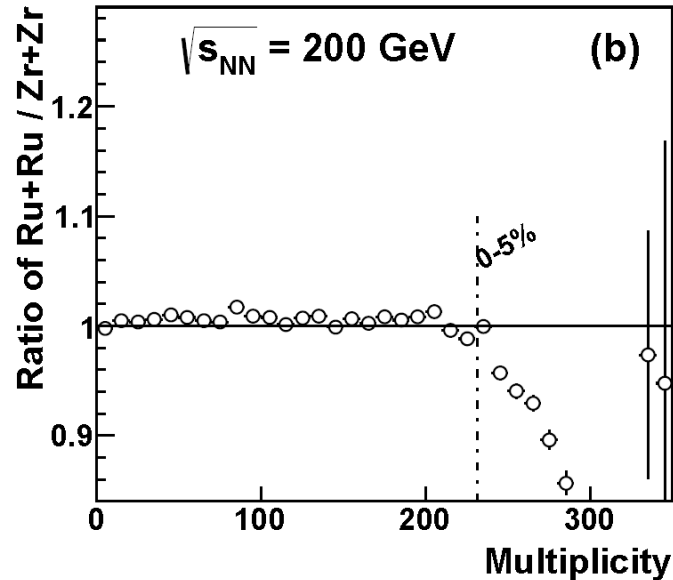
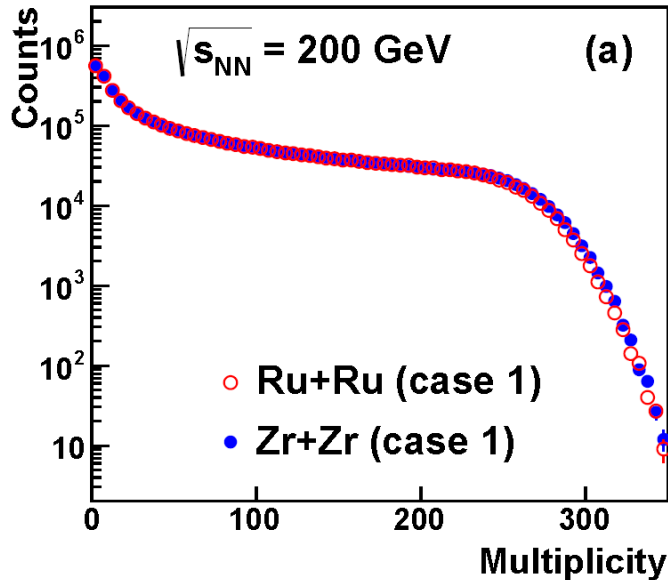
\longrightarrow CME contribution
changed

setting 1	R0	a(d)	β_2 <small>Radius^{Woods} (fm) & Deformation^{Woods}</small>	β_4
Ru96	5.0845	0.567	0.1579	0.00
Zr96	5.0212	0.574	0.08	0.00

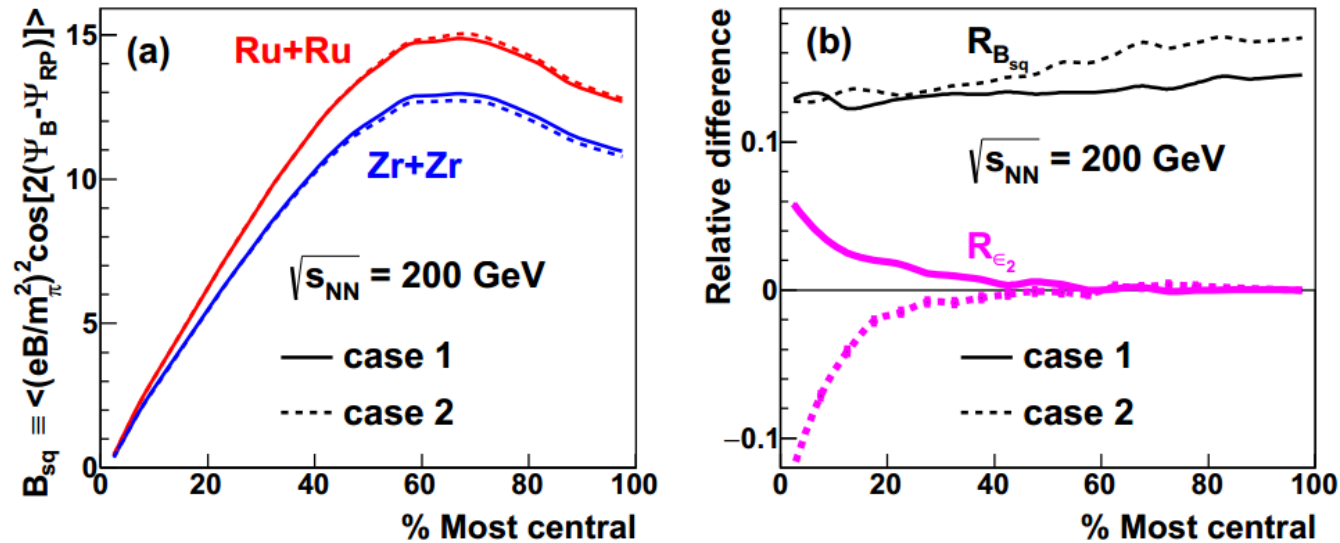
setting 2	R0	a(d)	β_2 <small>El.-Magn. properties</small>	β_4
Ru96	5.0845	0.567	0.053	0.009
Zr96	5.0212	0.574	0.217	0.01

Woods-Saxon density:

$$\rho(r, \theta) = \frac{\rho_0}{1 + e^{(r - R_0 + \beta_2 R_0 Y_2^0(\theta)) / a}}$$



Initial magnetic field and initial eccentricity



B_{sq} quantifies magnetic-field fluctuation

(Blozynski, Huang, Zhang, and Liao, 2013)

R is the relative difference: $2(RuRu - ZrZr) / (RuRu + ZrZr)$

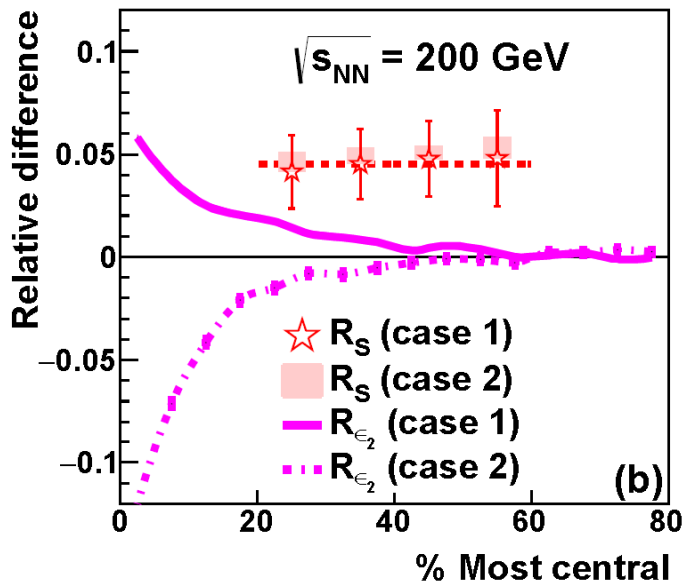
Centrality 20-60%: sizable difference in B ($R_{B_{sq}} \sim 10 - 20\%$)

but small difference in eccentricity ($R_{\epsilon_2} < 2\%$)

Results:

From Monte-Carlo simulation and fitting experiment data, we have: $bg = 2/3$

So, we can estimate the relative difference is about 5% for Ru+Ru and Zr+Zr

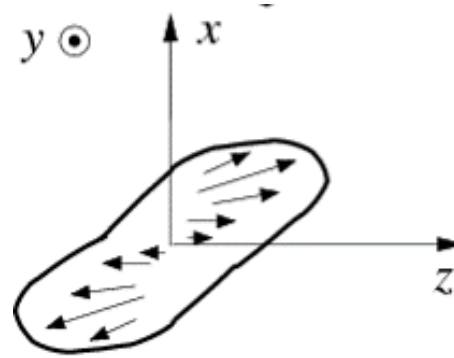
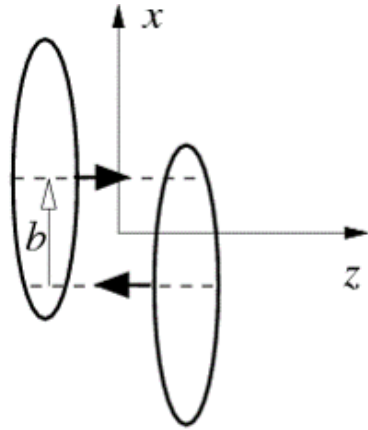


The systematic uncertainties are largely canceled out with the **relative difference** between Ru + Ru and Zr + Zr

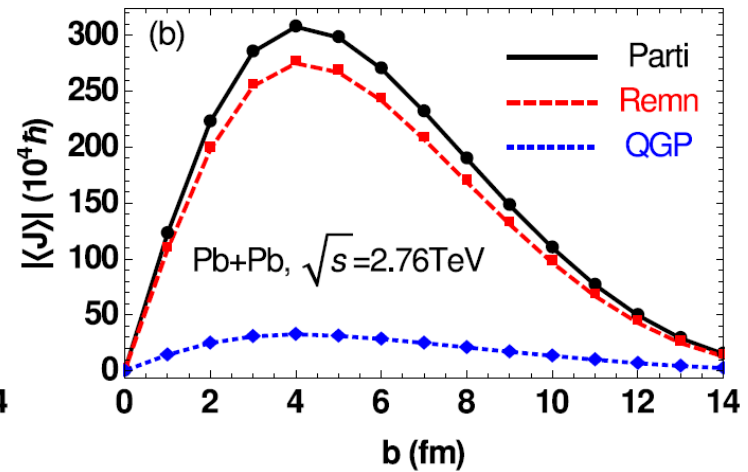
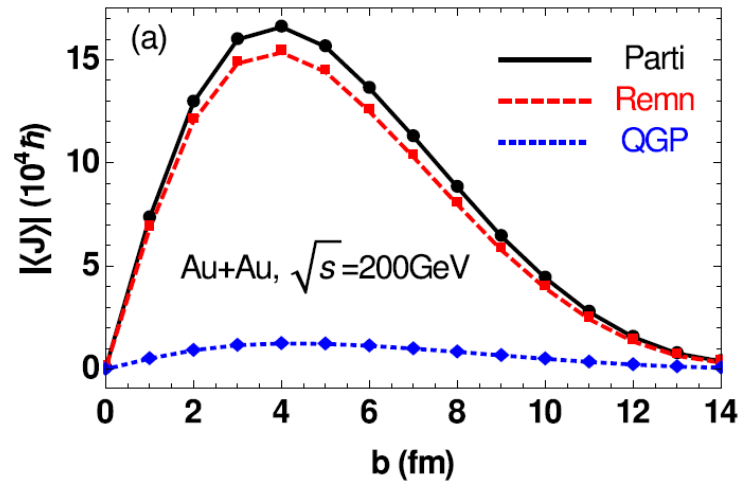
$$R_S = S^{Ru+Ru} - S^{Zr+Zr} = (N_{part} \Delta\gamma)^{Ru+Ru} - (N_{part} \Delta\gamma)^{Zr+Zr}$$

Vorticity in HIC


Total Orbital Angular Momentum in HIC



L_y



Total Orbital Angular Momentum in HIC

L_y  ?

Low energy
(nuclear binding energy)

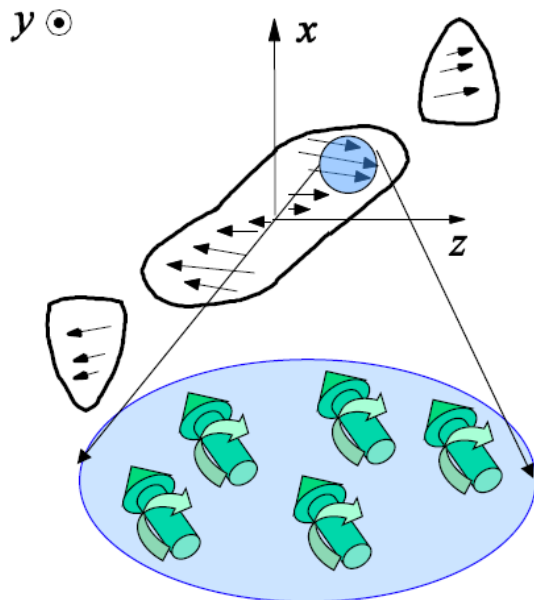


Rotating compound nucleus

High energy
(RHIC, LHC)



Shear of the longitudinal flow

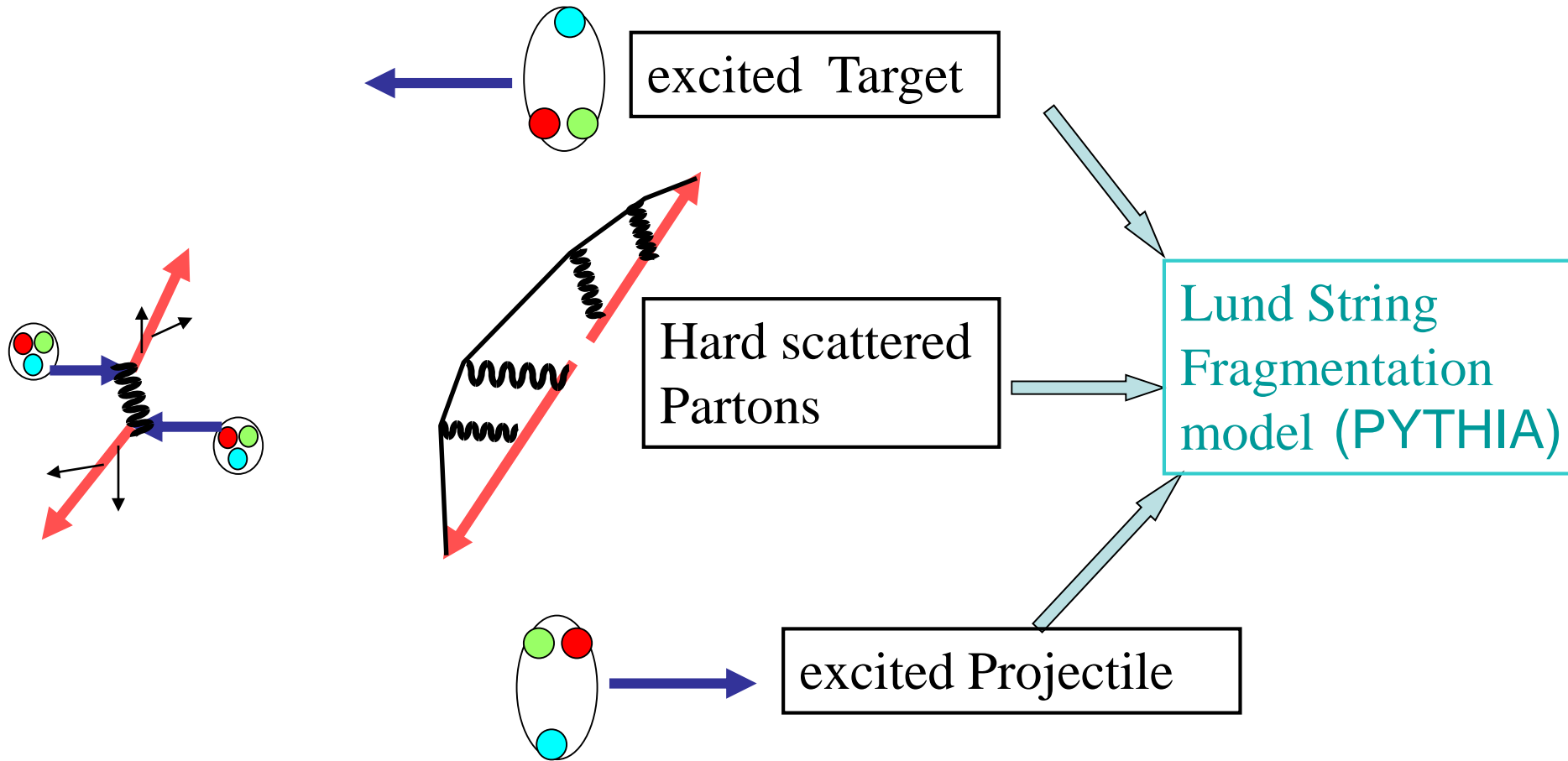


Local **vorticity**

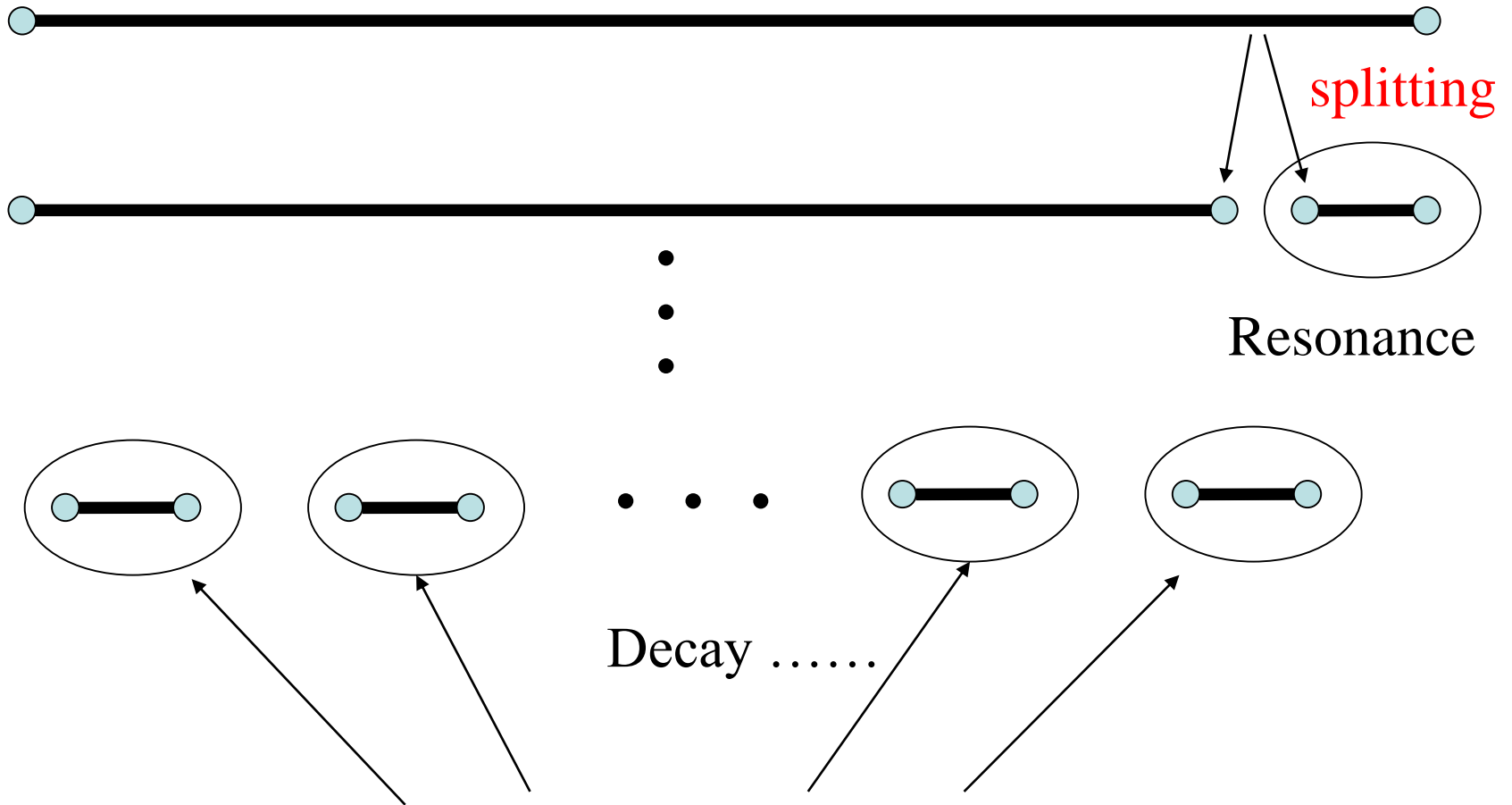


Quark global polarization

HIJING Model



Fragmentation process in HIJING (PYTHIA):



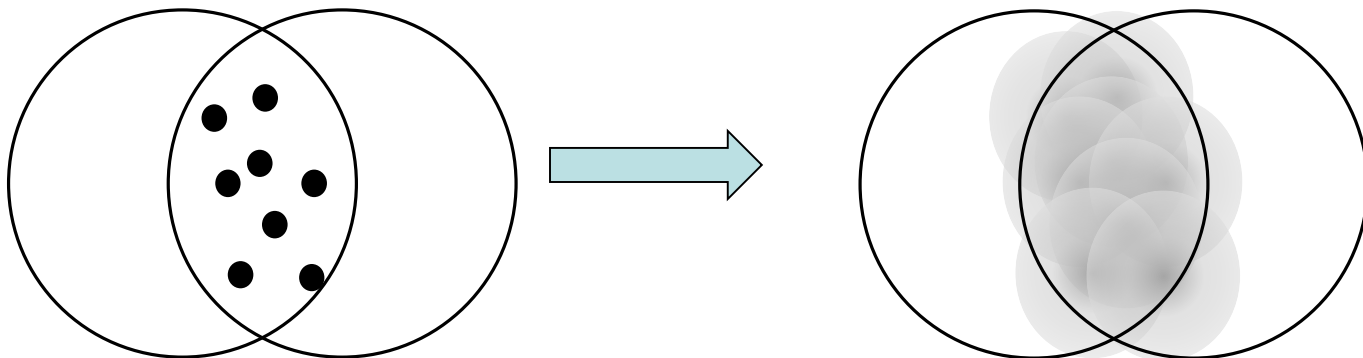
In this work: we decompose Resonances into partons

In order to get continuous distribution of velocity field, we introduce a smearing function:

$$\Phi_G(x, x_i) = \frac{K}{\tau_0 \sqrt{2\pi\sigma_\eta^2} 2\pi\sigma_r^2} \exp \left[-\frac{(x - x_i)^2 + (y - y_i)^2}{2\sigma_r^2} - \frac{(\eta - \eta_i)^2}{2\sigma_\eta^2} \right]$$

L. Pang, Q. Wang and X. N. Wang, Phys. Rev. C 86 (2012), 024911

With this smearing density function, the energy and momentum of each parton are represented by a wave packet, smearing into whole space

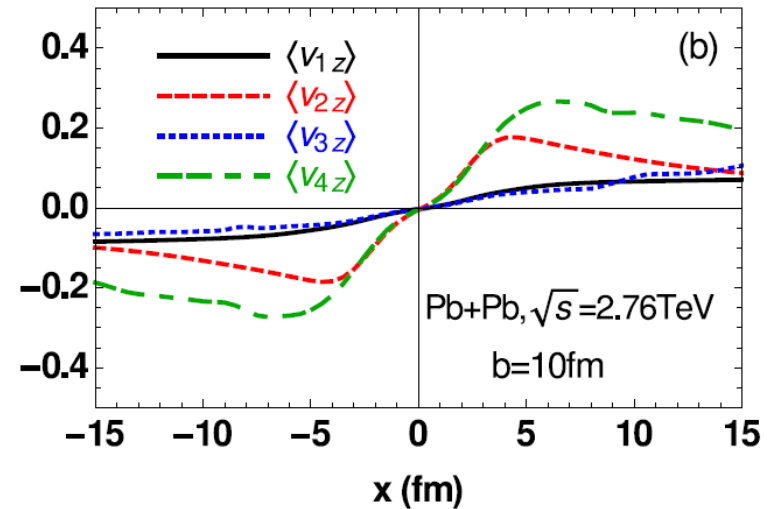
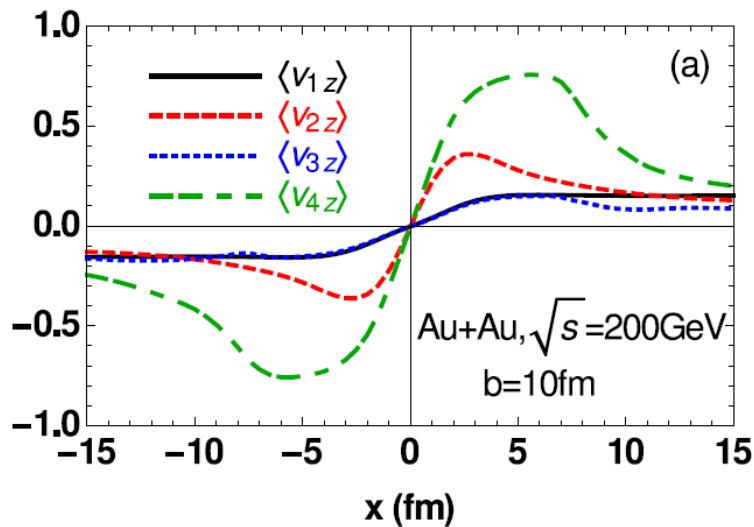


$$v_1^a(x) = \frac{1}{\sum_i \Phi(x, x_i)} \sum_i \frac{p_i^a}{p_i^0} \Phi(x, x_i),$$

——velocity of the particle flow

$$v_2^a(x) = \frac{\sum_i p_i^a \Phi(x, x_i)}{\sum_i [p_i^0 + (p_i^a)^2 / p_i^0] \Phi(x, x_i)},$$

——velocity of the energy flow

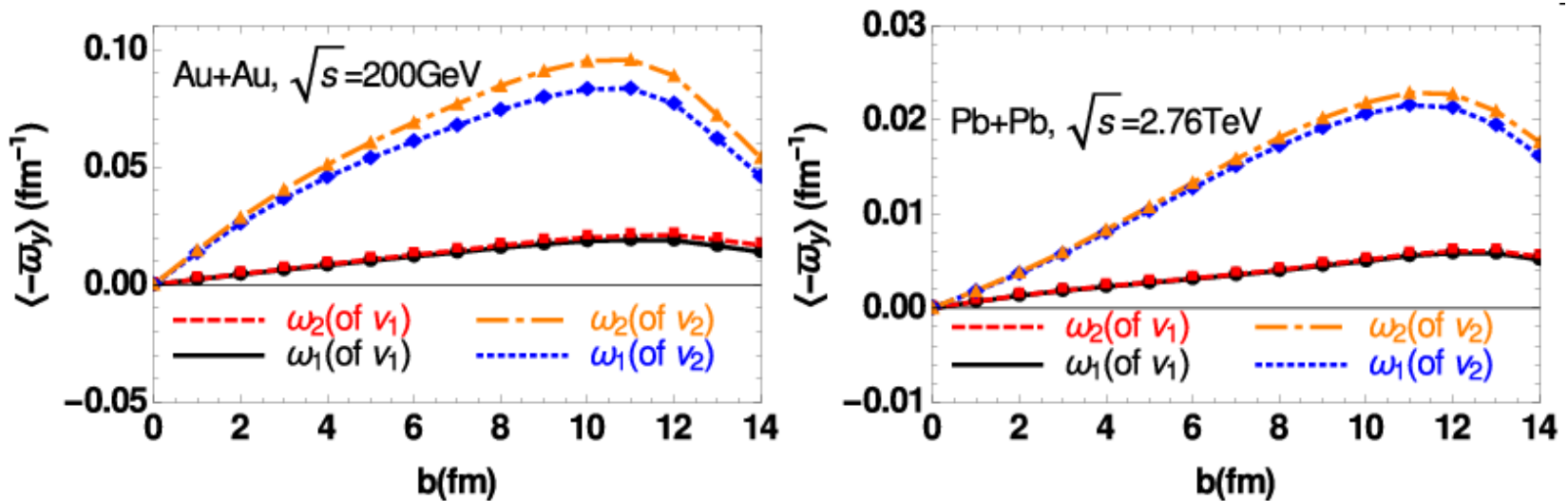


Definition of Vorticity

$\omega_1 = \nabla \times \mathbf{v}$, —the usual nonrelativistic definition

$\omega_2 = \gamma^2 \nabla \times \mathbf{v}$, —the spatial components of the relativistic definition

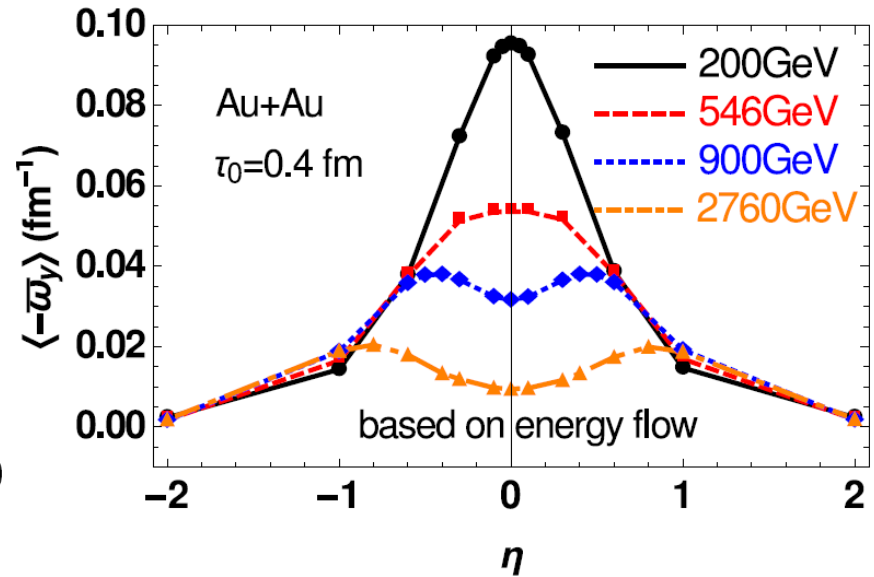
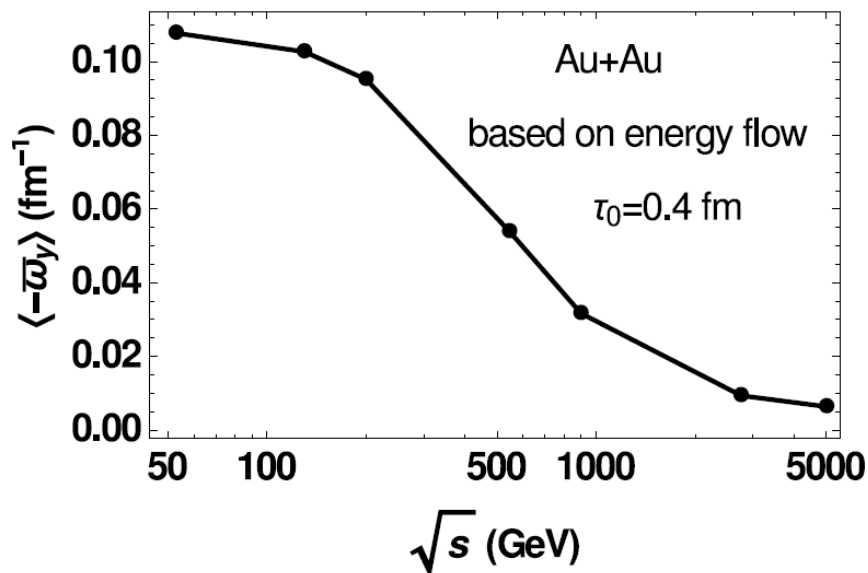
The space-averaged vorticity at τ_0 and $\eta=0$:



Most vortical fluid: Vorticity at 200GeV at $b=10$ fm is 10^{21} Hz.

(Fastest man-made rotation via laser light $\sim 10^7$ Hz)

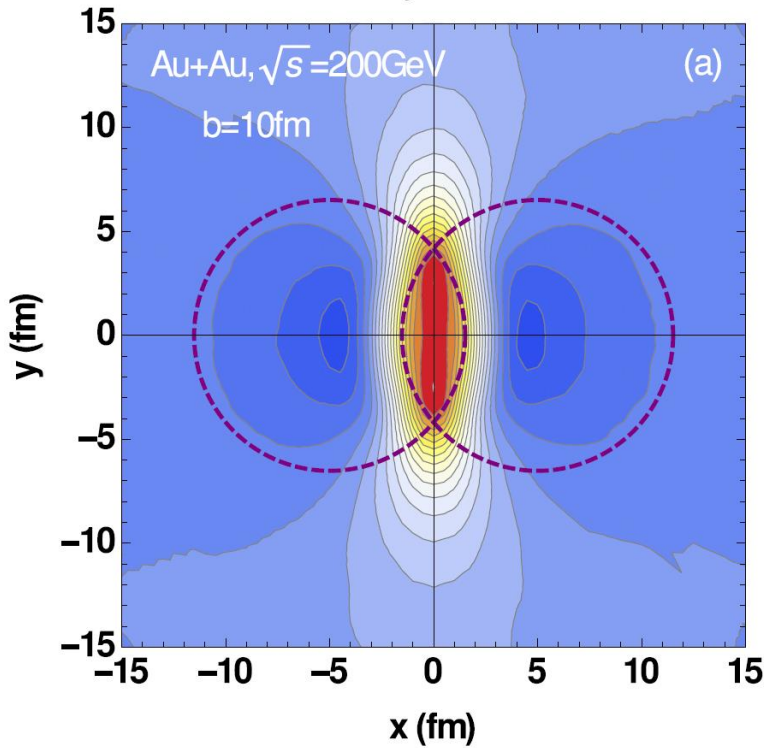
Collision energy dependence of Vorticity



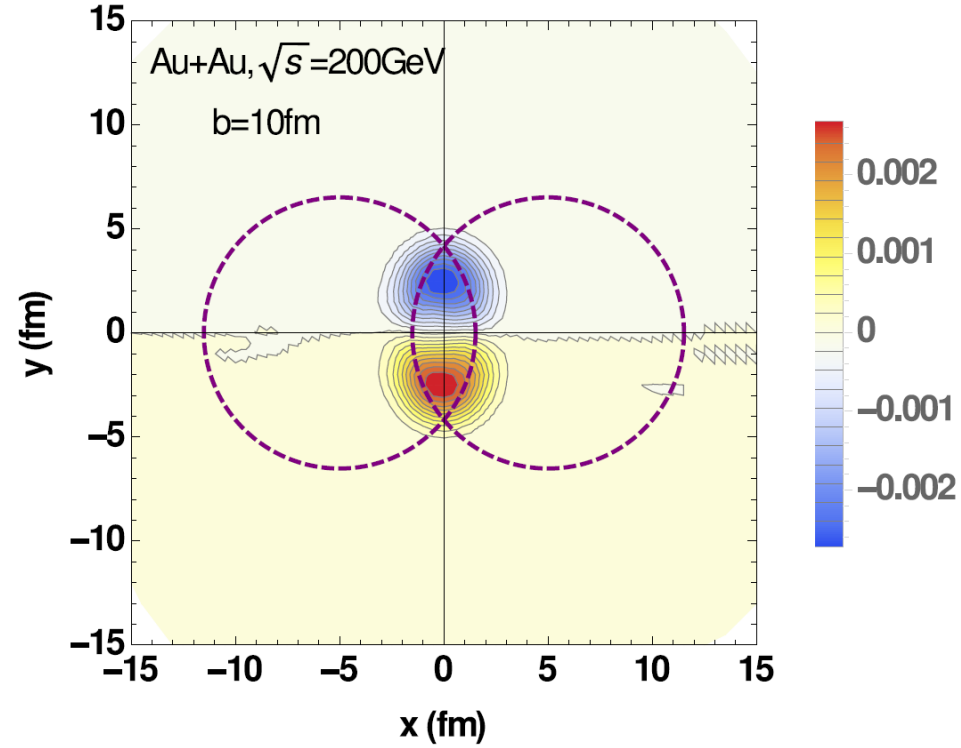
higher energy:
more AM carried by finite rapidity particles; mid-rapidity
closer to Bjorken boost invariant; larger moment of inertia

Spatial distribution of Vorticity

$\langle -\omega_{2y} \rangle$ (fm $^{-1}$)



$\langle T^2 \omega_2 \cdot v_2 \rangle$ (GeV 3)



Summary

- We have constructed a numerical framework for calculating the EM field and vorticity in HIC based on HIJING model
- We have investigated the generation and evolution of the EM fields in HIC on e-b-e events.
- Attempting to distinguish the background contribution and CME effect, we have surveyed two ways, including different size A+B collisions, and isobaric collisions.
- We have also simulated the generation of vorticity produced in HIC at initial stage.
- In the following study, we are concentrating on the evolution of this vorticity.
- The EM field produced in small system, p+p and p+A.